Homeostatic feedback, not early activity, modulates the development of two-state patterned activity in the *Caenorhabditis elegans* egg-laying behavior circuit

Short title: Development of *C. elegans* egg-laying circuit activity

Bhavya Ravi[1,2], Jessica Garcia[2], and Kevin M. Collins[1,2,3]

[1]Neuroscience Program, University of Miami Miller School of Medicine, Miami, FL USA

[2]Department of Biology, University of Miami, Coral Gables, FL USA

[3]To whom correspondence should be addressed:

kevin.collins@miami.edu

Department of Biology

University of Miami

1301 Memorial Drive

Coral Gables, FL 33143

Tel: (305) 284-9058

Website: www.bio.miami.edu/CollinsLab/

Twitter: @kevinemco

62 pages with 12 Figures and 6 Movies

Abstract- 242 words, Introduction- 647 words, Discussion- 1499 words.

Disclosures / Conflict of Interests

The authors declare that no competing interests exist. BR, JG, and KMC performed experiments and data analysis, and BR and KMC wrote the paper.

Acknowledgements

This work was funded by a grant from NINDS to KMC (R01 NS086932). JG was supported by the Bridge to the Baccalaureate Program (R25 GM050083). Strains used in this study have been provided to the *C. elegans* Genetics Center, which is funded by NIH Office of Research Infrastructure Programs (P40 OD010440). We thank Addys Bode and Michael Scheetz for technical assistance and help with strain construction. We thank James Baker, Julia Dallman, Laura Bianchi, Peter Larsson, Stephen Roper, and members of the Collins lab for helpful discussions and feedback.

Abstract

Neuron activity accompanies synapse formation and maintenance, but how early circuit activity contributes to behavior development is not well understood. Here, we use the *Caenorhabditis elegans* egg-laying motor circuit as a model to understand how coordinated cell and circuit activity develops and drives a robust two-state behavior in adults. Using calcium imaging in behaving animals, we find the serotonergic Hermaphrodite Specific Neurons (HSNs) and vulval muscles show rhythmic calcium transients in L4 larvae before eggs are produced. HSN activity in L4 is tonic and lacks the alternating burst-firing/quiescent pattern seen in egg-laying adults. Vulval muscle activity in L4 is initially uncoordinated but becomes synchronous as the anterior and posterior muscle arms meet at HSN synaptic release sites. However, coordinated muscle activity does not require presynaptic HSN input. Using reversible silencing experiments, we show that neuronal and vulval muscle activity in L4 is not required for the onset of adult behavior. Instead, the accumulation of eggs in the adult uterus renders the muscles sensitive to HSN input. Sterilization or acute electrical silencing of the vulval muscles inhibits presynaptic HSN activity, and reversal of muscle silencing triggers a homeostatic increase in HSN activity and egg release that maintains ~12-15 eggs in the uterus. Feedback of egg accumulation depends upon the vulval muscle postsynaptic terminus, suggesting a retrograde signal sustains HSN synaptic activity and egg release. Thus, circuit development and activity are necessary but not sufficient to drive behavior without additional modulation by sensory feedback.

52 **Key Words**

53 Neural circuit, development, *C. elegans*, calcium, serotonin, neuromodulation, behavior

54 **Significance Statement**

55 The functional importance of early, spontaneous neuron activity in synapse and circuit
56 development is not well understood. Here we show that in the nematode *C. elegans*, the
57 serotonergic Hermaphrodite Specific Neurons (HSNs) and postsynaptic vulval muscles
58 show activity during circuit development, well before the onset of adult behavior.
59 Surprisingly, early activity is not required for circuit development or the onset of adult
60 behavior, and the circuit remains unable to drive egg laying until fertilized embryos are
61 deposited into the uterus. Egg accumulation potentiates vulval muscle excitability, but
62 ultimately acts to promote burst firing in the presynaptic HSNs during which eggs are laid.
63 Our results suggest that mechanosensory feedback acts at three distinct steps to initiate,
64 sustain, and terminate *C. elegans* egg-laying circuit activity and behavior.

65

Introduction

Developing neural circuits in the cortex, hippocampus, cerebellum, retina, and spinal cord show spontaneous neural activity (Wong et al., 1995; Garaschuk et al., 1998; Garaschuk et al., 2000; Watt et al., 2009; Warp et al., 2012). In contrast, mature neural circuits show coordinated patterns of activity required to drive efficient behaviors. Activity-dependent mechanisms have been shown to play key roles during development in vertebrate neural circuits (Gu et al., 1994; Gu and Spitzer, 1995; Jarecki and Keshishian, 1995; Borodinsky et al., 2004; Hanson et al., 2008), but the complexity of such circuits poses limitations in terms of understanding how developmental events, neurotransmitter expression, and sensory signals act together to promote the transition from immature to mature patterns of circuit activity. Genetically tractable invertebrate model organisms, such as the nematode *Caenorhabditis elegans*, have simple neural circuits and are amenable to powerful experimental approaches allowing us to investigate how activity in neural circuits is shaped during development.

The *C. elegans* egg laying circuit is a well-characterized neural circuit that drives a two-state behavior in adult animals with ~20 minute inactive periods punctuated by ~2 minute active states where ~4-6 eggs are laid (Waggoner et al., 1998). The egg-laying circuit comprises two serotonergic Hermaphrodite Specific Neurons (HSNs) which promote the active state (Waggoner et al., 1998; Emtage et al., 2012), three locomotion motor neurons (VA7, VB6, and VD7) which may drive rhythmic input into the circuit (Collins et al., 2016), and six cholinergic Ventral C neurons (VC1-6), all of whom synapse onto a set of vulval muscles that contract to allow release eggs from the uterus (White et al., 1986). Four uv1 neuroendocrine cells connect the vulval canal to the uterus which

89 holds embryos until they are laid. HSN, VC, uv1, and vulval muscle development occurs
90 during the early-mid L4 larval stages and requires interactions with the developing vulval
91 epithelium, but not the other cells in the circuit (Colavita and Tessier-Lavigne, 2003; Shen
92 and Bargmann, 2003; Shen et al., 2004).

93 During egg laying, serotonin released from the HSNs signals through vulval muscle
94 receptors (Carnell et al., 2005; Dempsey et al., 2005; Hobson et al., 2006; Dernovici et
95 al., 2007; Hapiak et al., 2009), likely increasing the excitability of the muscles so that
96 rhythmic input from cholinergic motor neurons can drive vulval muscle contractions (White
97 et al., 1986; Collins and Koelle, 2013; Collins et al., 2016). We have previously shown
98 that HSN Ca^{2+} transients occur more frequently during the active state, but the factors
99 which promote this timely 'feed-forward' increase in HSN activity remain poorly
100 understood. The cholinergic VCs show rhythmic Ca^{2+} transients coincident with vulval
101 muscle contractions during the active state, although whether VC activity drives
102 contraction itself or instead acts to modulate HSN signaling is still not clear (Schafer et
103 al., 1996; Bany et al., 2003; Ringstad and Horvitz, 2008; Zang et al., 2017). The uv1 cells,
104 mechanically deformed by the passage of eggs through the vulva, release tyramine and
105 neuropeptides that signal extrasynaptically to inhibit HSN activity (Collins et al., 2016;
106 Banerjee et al., 2017). Because each cell in the circuit develops independently in
107 juveniles, how this circuit goes on to develop the robust pattern of coordinated activity
108 seen in adults remains unclear.

109 We show here the presynaptic HSN motor neurons and the postsynaptic vulval
110 muscles are active during the late L4 larval stage, well before egg production and the
111 onset of adult egg-laying behavior. We do not observe activity in the VC neurons and uv1

112 neuroendocrine cells until behavioral onset. The adult circuit remains in a non-functional
113 state until receiving feedback of eggs in the uterus. This egg-laying homeostat requires
114 the vm2 muscle arms and muscle activity which we show promotes HSN burst firing that
115 maintains the active state. Together, our data reveal how cell activity patterns that emerge
116 during circuit development are modulated by sensory feedback that decide when and for
117 how long to drive behavior.

118

119 **Materials and Methods**

120

121 **Nematode Culture and Developmental Staging**

122 *Caenorhabditis elegans* hermaphrodites were maintained at 20°C on Nematode Growth
123 Medium (NGM) agar plates with *E. coli* OP50 as a source of food as described (Brenner,
124 1974). Animals were staged and categorized based on the morphology of the vulva as
125 described (Mok et al., 2015). For assays involving young adults, animals were age-
126 matched based on the timing of completion of the L4 larval molt. All assays involving adult
127 animals were performed using age-matched adult hermaphrodites 20-40 hours past the
128 late L4 stage.

129

130 **Plasmid and strain construction**

131 Calcium reporter transgenes

132 ***Vulval Muscle Ca^{2+}:*** To visualize vulval muscle Ca^{2+} activity in adult animals, we used
133 LX1918 *vsIs164* [*unc-103e::GCaMP5::unc-54 3'UTR + unc-103e::mCherry::unc-54*
134 *3'UTR + lin-15(+)*] *lite-1(ce314) lin-15(n765ts) X* strain as described (Collins et al., 2016).

135 In this strain, GCaMP5G (Akerboom et al., 2013) and mCherry are expressed from the
136 *unc-103e* promoter (Collins and Koelle, 2013). The *unc-103e* promoter is only weakly
137 expressed in vulval muscles during the L4 stages. To visualize vulval muscle activity in
138 L4 animals, we expressed GCaMP5G and mCherry from the *ceh-24* promoter (Harfe and
139 Fire, 1998). A ~2.8 kB DNA fragment upstream of the *ceh-24* start site was amplified from
140 genomic DNA by PCR using the following oligonucleotides: 5'-GCG GCA TGC AAC GAG
141 CCA TCC TAT ATC GGT GGT CCT CCG-3' and 5'-CAT CCC GGG TTC CAA GGC AGA
142 GAG CTG CTG-3'. This DNA fragment was ligated into pKMC257 (mCherry) and
143 pKMC274 (GCaMP5G) from which the *unc-103e* promoter sequences were excised to
144 generate pBR3 and pBR4, respectively. pBR3 (20 ng/µl) and pBR4 (80 ng/µl) were
145 injected into LX1832 *lite-1(ce314) lin-15(n765ts) X* along with the pLI5EK rescue plasmid
146 (50 ng/µl) (Clark et al., 1994). The extrachromosomal transgene produced was integrated
147 by irradiation with UV light after treatment with trimethylpsoralen (UV/TMP) creating two
148 independent transgenes *keyIs12* and *keyIs13*, which were then backcrossed to LX1832
149 parental line six times to generate the strains MIA51 and MIA53. Strain MIA51 *keyIs12*
150 [*ceh-24::GCaMP5::unc-54 3'UTR + ceh-24::mCherry::unc-54 3'UTR + lin-15(+)*] *IV*; *lite-*
151 *1(ce314) lin-15 (n765ts) X* was subsequently used for Ca^{2+} imaging. We noted repulsion
152 between *keyIs12* and *wzIs30 IV*, a transgene that expresses Channelrhodopsin-2::YFP
153 in HSN from the *egl-6* promoter (Emtage et al., 2012), suggesting both were linked to
154 chromosome IV. As a result, we crossed MIA53 *keyIs13* [*ceh-24::GCaMP5::unc-54*
155 *3'UTR + ceh-24::mCherry::unc-54 3'UTR + lin-15(+)*]*; lite-1(ce314) lin-15(n765ts) X* with
156 LX1836 *wzIs30 IV*; *lite-1(ce314) lin-15(n765ts) X*, generating MIA88 which was used to
157 activate HSN neurons and record vulval muscle Ca^{2+} in L4 animals. In the case of young

158 adults (3.5 & 6.5h post molt) and 24h old adults, strain LX1932 *wzIs30 IV; vsIs164 lite-*
159 *1(ce314) lin-15(n765ts) X* was used as described (Collins et al., 2016).
160 ***HSN Ca^{2+}:*** To visualize HSN Ca^{2+} activity in L4 and adult animals, we used the LX2004
161 *vsIs183* [*nlp-3::GCaMP5::nlp-3 3'UTR + nlp-3::mCherry::nlp-3 3'UTR + lin-15(+)*] *lite-*
162 *1(ce314) lin-15(n765ts) X* strain expressing GCaMP5G and mCherry from the *nlp-3*
163 promoter as previously described (Collins et al., 2016). In order to visualize HSN Ca^{2+}
164 activity in *lin-12(wy750)* mutant animals lacking post-synaptic vm2 vulval muscle arms,
165 we crossed the MIA194 *lin-12(wy750) III* with LX2004 *vsIs183 lite-1(ce314) lin-15(n765ts)*
166 *X* to generate MIA196 *lin-12(wy750) III*; *vsIs183 X lite-1(ce314) lin-15 (n765ts) X.*
167
168 Histamine gated chloride channel (HisCl) expressing transgenes
169 ***Vulval muscle HisCl:*** To produce a vulval muscle-specific HisCl transgene, coding
170 sequences for mCherry in pBR3 were replaced with that for HisCl. First, an EagI
171 restriction site (3' of the mCherry encoding sequence) was changed to a NotI site using
172 Quickchange site-directed mutagenesis to generate pBR5. The ~1.2 kB DNA fragment
173 encoding the HisCl channel was amplified from pNP403 (Pokala et al., 2014) using the
174 following oligonucleotides: 5'- GCG GCT AGC GTA GAA AAA ATG CAA AGC CCA ACT
175 AGC AAA TTG G-3' and 5'-GTG GCG GCC GCT TAT CAT AGG AAC GTT GTC-3', cut
176 with NheI/NotI, and ligated into pBR5 to generate pBR7. pBR7 (80 ng/µl) was injected
177 into LX1832 along with pLI5EK (50 ng/µl). One line bearing an extrachromosomal
178 transgene was integrated with UV/TMP, and six independent integrants (*keyIs14* to
179 *keyIs19*) were recovered. Four of these were then backcrossed to the LX1832 parental
180 line six times to generate strains MIA68, MIA69, MIA70, and MIA71. All four strains were

181 used for behavioral assays in adult animals to test the effect of vulval muscle silencing on
182 egg laying (Fig. 6B). MIA71 *keyIs19* [*ceh-24::HisCl::unc-54 3'UTR* + *lin-15(+)*]*; lite-*
183 *1(ce314) lin-15(n765ts) X* strain was used to study the effect of acute silencing of early
184 activity on egg-laying behavior (Fig. 6C). To visualize HSN Ca^{2+} activity after vulval
185 muscle silencing, we crossed MIA71 with LX2004 to generate strain MIA80 *keyIs19;*
186 *vsIs183 lite-1(ce314) lin-15(n765ts) X.*
187 ***HSN HisCl:*** The ~1.2 kB DNA fragment encoding the HisCl channel was amplified from
188 pNP403 using the following oligonucleotides: 5'- GCG GCT AGC GTA GAA AAA ATG
189 CAA AGC CCA ACT AGC AAA TTG G-3' and 5'-GCG GAG CTC TTA TCA TAG GAA
190 CGT TGT CCA ATA GAC AAT A-3'. The amplicon was digested with NheI/SacI and
191 ligated into similarly cut pSF169 (*pegl-6*::mCre (Flavell et al., 2013)) to generate pBR10.
192 To follow expression in HSN, mCherry was amplified using the following oligonucleotides:
193 5'- GCG GCT AGC GTA GAA AAA ATG GTC TCA AAG GGT-3' and 5'- GCG GAG CTC
194 TCA GAT TTA CTT ATA CAA TTC ATC CAT G-3'. This amplicon was digested with
195 NheI/SacI and ligated into pSF169 to generate pBR12. pBR10 (HisCl; 5 ng/µl) and pBR12
196 (mCherry; 10 ng/µl) were injected into LX1832 *lite-1(ce314) lin-15(n765ts)* along with
197 pLI5EK (50 ng/µl). The extrachromosomal transgene produced was integrated with
198 UV/TMP, creating three independent integrants (*keyIs20, keyIs21, and keyIs22*). The
199 resulting animals were backcrossed to the LX1832 parental line six times to generate
200 strains MIA115, MIA116, and MIA117. The MIA116 strain had a low incidence of HSN
201 developmental defects and was used subsequently for behavioral assays.
202 ***All neuron HisCl:*** pNP403 was injected into LX1832 *lite-1(ce314) lin-15(n765ts)* animals
203 at 50 ng/µl along with pLI5EK (50 ng/µl) to produce strain MIA60 carrying

204 extrachromosomal transgene *keyEx16* [*tag-168::HisCl::SL2::GFP + lin15(+)*]. Non-Muv,
205 *lin-15(+)* animals with strong GFP expression in the HSNs and other neurons were
206 selected prior to behavioral silencing assays. All animals showed histamine-dependent
207 paralysis that recovered after washout.
208
209 Transgenic reporters of circuit development and morphology
210 ***Vulval muscle morphology:*** To visualize vulval muscle development at the L4 stages,
211 we injected pBR3 [*pceh-24*::mCherry] (80 ng/µl) along with a co-injection marker pCFJ90
212 (10 ng/µl) into TV201 *wyIs22* [*punc-86*::GFP::RAB-3 + *podr-2*::dsRed] (Patel et al., 2006)
213 to generate an extrachromosomal transgene, *keyEx42*. To visualize adult vulval muscle
214 morphology, we used the LX1918 *vsIs164* [*unc-103e::GCaMP5::unc-54 3'UTR + unc-*
215 *103e::mCherry::unc-54 3'UTR + lin-15(+)*] *lite-1(ce314) lin-15(n765ts) X* strain (Collins et
216 al., 2016). To visualize the expression of the *ser-4* gene, we used the strain AQ570
217 [*ijIs570*] (Tsalik and Hobert, 2003; Gurel et al., 2012).
218 ***HSN morphology:*** We used the LX2004 strain expressing mCherry from the *nlp-3*
219 promoter to visualize HSN morphology at L4 stages as well as in adults. To visualize
220 GFP::RAB-3 synaptic localization in HSNs during development, the *wyIs22* transgene
221 was used (Patel et al., 2006).
222 ***Whole circuit morphology (HSN, VC and uv1 cells):*** A ~3.2 kB DNA fragment
223 upstream of the *ida-1* start site (Cai et al., 2004) was cloned using the following
224 oligonucleotides: 5'-GCG GCA TGC CCT GCC TGT GCC AAC TTA CCT-3' and 5'-CAT
225 CCC GGG GCG GAT GAC ACA GAG ATG CGG-3'. The DNA fragment was digested
226 with SphI/XmaI and ligated into pKMC257 and pKMC274 to generate plasmids pBR1 and

227 pBR2. pBR1 (20 ng/µl) and pBR2 (80 ng/µl) were co-injected into LX1832 along with
228 pLI5EK (50 ng/µl). The extrachromosomal transgene produced was integrated with
229 UV/TMP creating four independent integrants *keyIs8* to *keyIs11,* which were then
230 backcrossed to LX1832 parental line six times. MIA49 *keyIs11* [*ida-1::GCaMP5::unc-54*
231 *3'UTR + ida-1::mCherry::unc-54 3'UTR + lin-15(+)*]; *lite-1(ce314) lin-15 (n765ts) X* was
232 used subsequently to visualize whole-circuit morphology.

233 **Confocal Microscopy and Ratiometric Ca^{2+} Imaging**

234 To visualize the egg-laying system, L4s and age-matched adults were immobilized using
235 10 mM muscimol on 4% agarose pads and covered with #1 coverslips. Two-channel
236 confocal Z-stacks (along with a bright-field channel) using a pinhole opening of 1 Airy Unit
237 (0.921 µm thick optical sections, 16-bit images) were obtained with an inverted Leica TCS
238 SP5 confocal microscope with a 63X Water Apochromat objective (1.2NA). Ca^{2+}
239 recordings were made using the 8 kHz resonant scanner and the pinhole opened for ~20
240 µm optical slices. Recordings were collected at ~20 fps at 256x256 pixel resolution, 12-
241 bit depth and ≥2X digital zoom using a 20x Apochromat objective (0.7 NA).
242 GFP/GCaMP5G and mCherry fluorescence was excited using a 488 nm and 561 nm laser
243 lines, respectively. L4 animals at the relevant stages of vulval development were identified
244 based on vulval morphology (Mok et al., 2015). Adult recordings were performed 24 hours
245 after the late L4 stage. Young adults (3.5–6.5 h) were staged after cuticle shedding at the
246 L4 to adult molt. After staging, animals were allowed to adapt for ~30 min before imaging.
247 During imaging, the stage and focus were adjusted manually to keep the relevant cell/pre-
248 synapse in view and in focus.

249 Ratiometric analysis (GCaMP5:mCherry) for all Ca^{2+} recordings was performed
250 after background subtraction using Volocity 6.3.1 (Perkin Elmer) as described (Collins et
251 al., 2016; Ravi et al., 2018). The egg-laying active state was operationally defined as the
252 period one minute prior to the first egg-laying event and ending one minute after the last
253 (in the case of a typical active phase where 3-4 eggs are laid in quick succession).
254 However, in cases where two egg-laying events were apart by >60 s, peaks were
255 considered to be in separate active phases and transients between these were
256 considered to be from the inactive state.

257 ***Ratiometric Ca^{2+} comparisons with different reporters and developmental stages.***
258 To facilitate comparisons of ΔR/R between different reporters at different developmental
259 stages, particularly during periods of elevated Ca^{2+} activity, HSN recordings in which
260 baseline GCaMP5/mCherry fluorescence ratio values were between 0.2-0.3 were
261 selected for the analysis, while vulval muscle recordings with GCaMP5/mCherry ratio
262 values between 0.1-0.2 were chosen (≥80% of recordings). Because HSN Ca^{2+} transient
263 amplitude did not change significantly across developmental stages or in mutant
264 backgrounds, most our analyses focused on HSN Ca^{2+} transient frequency. To test
265 whether vulval muscle Ca^{2+} transient amplitudes recorded using different transgenes
266 were suitable for quantitative comparisons, we measured the average GCaMP5:mCherry
267 fluorescence ratio from two 15 by 15 µm regions of interest (ROI) from the anterior and
268 posterior vulval muscles under identical imaging conditions (data not shown). The ROIs
269 were positioned so as to ensure maximal coverage of the muscle cell area. We found that
270 resting GCaMP5:mCherry ratios (±95% confidence intervals) bearing either the *ceh-24*
271 (*keyIs12*) or *unc-103e* (*vsIs164*) vulval muscle Ca^{2+} reporter transgenes were not

272 statistically different at the developmental stages under comparison in Fig. 4H (L4.7-8
273 *(ceh-24)*: 1.055 ±0.027; L4.9 *(ceh-24)*: 1.055 ±0.0605; Adult *(unc-103e)*: 1.15 ±0.064;
274 n≥10 animals measured per developmental stage). The coordination of vulval muscle
275 contraction was determined as described (Li et al., 2013).

276 ***ERG expression analysis.*** To assess *C. elegans* ERG (*unc-103e*) expression in the
277 vulval muscles during development, we used identical imaging conditions to measure
278 mCherry fluorescence (±95% confidence intervals) in animals bearing the *unc-103e*
279 (*vsIs164*) vulval muscle Ca^{2+} reporter transgene in the L4.7-8 and L4.9 larvae and in 24-
280 hour adults. We measured average mCherry fluorescence from two 15 by 15 µm ROI
281 placed on the anterior and posterior vulval muscles, as indicated above. A control ROI
282 was placed outside of the animal was used for fluorescence background subtraction.

283

284 **Behavior Assays and Microscopy**

285 ***Optogenetics and Defecation Behavior Assays:*** ChR2 expressing strains were
286 maintained on OP50 with or without all-*trans* retinal (ATR) (0.4 mM). ChR2 was activated
287 during Ca^{2+} imaging experiments with the same, continuous laser light used to excite
288 GCaMP5 fluorescence. Intervals between Expulsion steps of the defecation motor
289 program were determined as described from brightfield and HSN Ca^{2+} recordings
290 (Thomas, 1990). To test whether optogenetic activation of the HSNs affected defecation
291 behavior on plates, a OTPG_4 TTL Pulse Generator (Doric Optics) was used to trigger
292 image capture (Grasshopper 3, 4.1 Megapixel, USB3 CMOS camera, Point Grey
293 Research) and shutter opening on a EL6000 metal halide light source generating 8-16
294 mW/cm^2 of ~470±20nm blue light via a EGFP filter set mounted on a Leica M165FC

295 stereomicroscope. Late L4 and adult LX1836 transgenic animals were maintained on
296 OP50 seeded with or without all-*trans* retinal (ATR) (0.4 mM). Animals were illuminated
297 with continuous blue light for a duration of 2 minutes, and video recordings were analyzed
298 to identify the timing of defecation events within the duration of blue light activation.

299 ***Acute silencing experiments using HisCl:*** For acute silencing assays, NGM plates
300 containing 10 mM histamine were prepared and used as described (Pokala et al., 2014).
301 For adult behavioral assays, HisCl expressing strains were staged as late L4s with assays
302 performed 24 hours later. For L4 activity silencing, L4.7 animals were placed on NGM
303 plates with or without 10 mM histamine and were monitored to note when the animals
304 complete the L4 molt. Each animal was then transferred to a new seeded plate, and the
305 time for each animal to lay its first egg was recorded.

306 ***Animal sterilization using Floxuridine (FUDR):*** Animals were sterilized using
307 Floxuridine (FUDR). 100 µl of 10 mg/ml FUDR was applied to OP50 seeded NGM plates.
308 Late L4 animals were then staged onto the FUDR plates and the treated adults were
309 imaged 24 hours later.

310

311 **Experimental Design and Statistical Analysis**.

312 Sample sizes for behavioral assays followed previous studies (Chase et al., 2004; Collins
313 and Koelle, 2013; Collins et al., 2016). No explicit power analysis was performed before
314 the study. Statistical analysis was performed using Prism 6 (GraphPad). Ca^{2+} transient
315 peak amplitudes, widths, and inter-transient intervals were pooled from multiple animals
316 (typically ~10 animals per genotype/condition per experiment). No animals or data were

317 excluded. Individual *p* values are indicated in each Figure legend, and all tests were
318 corrected for multiple comparisons (Bonferroni for ANOVA; Dunn for Kruskal-Wallis).
319

320 **Results**

321 **Asynchronous presynaptic and postsynaptic development in the *C. elegans* egg-**
322 **laying behavior circuit**

323 We have previously described the function of cell activity in the adult egg-laying
324 behavior circuit and how developmental mutations impact circuit activity and adult
325 behavior (Collins and Koelle, 2013; Li et al., 2013; Collins et al., 2016). Because
326 development of the cells in the circuit is complete by the end of the fourth larval (L4) stage
327 (Li and Chalfie, 1990), we wanted to determine the relationship between cell activity and
328 circuit development in juveniles and compare early activity to that seen in egg-laying
329 adults. We exploited the stereotyped morphology of the developing primary and
330 secondary vulval epithelial cells in the fourth (final) larval stage to define discrete half-
331 hour stages of development as described (Mok et al., 2015). Fig. 1A-D shows vulval
332 morphologies during the transition from L4.7 to L4.9 just prior to the L4-adult molt. The
333 L4.7-8 larval transition lasted for ~1 hour, transitioning into the L4.8 ~0.5 h after Fig. 1B
334 (right panel). The vulval lumen began to shrink in L4.8 and was fully collapsed by L4.9,
335 ~0.5 h later (Fig. 1C-D) (Mok et al., 2015). Vulval development was complete at the time
336 of the final molt (Fig. 1E), and a fully formed vulva could be seen after cuticle shedding
337 (Fig. 1F).

338 We find that HSN morphological and pre-synaptic development is complete prior
339 to the late L4 larval stages, confirming previous observations with light microscopy and
340 serial electron microscopy reconstruction (Shen and Bargmann, 2003; Shen et al., 2004;
341 Adler et al., 2006; Patel et al., 2006). We expressed mCherry in HSNs from the NLP-3
342 neuropeptide promoter. We confirmed that the HSN axon had fasiculated and developed
343 enlarged anterior and posterior synaptic boutons in L4.7-8 and L4.9 animals (arrowheads
344 in Fig. 1G and H). This organization is nearly identical to the HSN morphology seen in
345 adults except that we sometimes detect a dorsal extension in adult animals that develops
346 toward the position of the uv1 neuroendocrine cells (third arrowhead in Fig. 1I).
347 GFP::RAB-3 expressed in HSN from the *unc-86* promoter showed clear punctate
348 localization at synaptic sites in late L4 animals (Fig. 1J and K), similar to that seen in
349 adults (Fig. 1L), suggesting that HSN presynaptic development is largely complete by
350 L4.7-8.

351 Unlike HSNs, we found the post-synaptic vulval muscles completed their
352 morphological development during the L4.9 stage, just prior to the L4 molt. We expressed
353 mCherry in the vulval muscles from the *ceh-24* promoter (Harfe and Fire, 1998) and found
354 that the vm1 and vm2 vulval muscles were still developing at the L4.7-8 stage (Fig. 1M).
355 After lumen collapse at the L4.9 stage, the tips of the vm1 muscles extended ventrally to
356 the lips of the vulva, and the anterior and posterior vm2 muscle arms extended laterally
357 along the junction between the primary and secondary vulval epithelial cells (Fig. 1N),
358 making contact with each other at the HSN (and VC) synaptic release sites that continues
359 in adults (Fig. 1O). Previous work has shown that mutations that disrupt LIN-12/Notch

360 signaling perturb development of the vm2 muscle arms in late L4 animals, during the time
361 when we observed vm2 muscle arm extension (Li et al., 2013).

362 Vulval muscles express multiple receptors that might respond to serotonin
363 released from HSN (Carnell et al., 2005; Dempsey et al., 2005; Hobson et al., 2006;
364 Dernovici et al., 2007; Hapiak et al., 2009). In order to look at the developmental
365 expression pattern of one such serotonin receptor, we examined a transgenic reporter
366 line expressing GFP under the *ser-4b* gene promoter (Tsalik and Hobert, 2003; Gurel et
367 al., 2012). As shown in Fig. 1P and 1Q, we observed strong GFP expression in VulF and
368 VulE primary and VulD secondary epithelial cells (Shen et al., 2004; Li et al., 2013). The
369 *ser-4b* promoter also drove weak GFP expression in the vm2 muscles in L4.7-9, and this
370 was elevated in adults (Fig. 1P-R). Serial EM reconstruction has shown that HSN makes
371 transient synapses onto the vulval epithelial cells in developing L4 animals (Shen et al.,
372 2004). Lastly, we wanted to determine whether the VC motor neurons and uv1
373 neuroendocrine cells had completed their development in late L4 animals. To
374 simultaneously visualize HSN, VC, and the uv1 neuroendocrine cells, we expressed
375 mCherry from the *ida-1* promoter, a gene expressed in a subset of peptidergic cells,
376 including those in the egg-laying circuit (Cai et al., 2004). As expected, HSN and VC
377 presynaptic termini assembled at the junction between the primary and secondary vulval
378 epithelial cells in L4.7-8. The uv1 cells were positioned laterally to the HSN/VC synaptic
379 regions and extended dorsal processes around the primary vulval epithelial cells (Fig.1S-
380 U). These results indicate that the morphological development of the HSN, VC, and uv1
381 cells is largely complete by L4.7-8 stage. In contrast, vulval muscle development

382 continues until after the L4.9 stage when the vm2 muscle arms reach each other and the
383 HSN and the VC presynaptic boutons.

384 **HSNs switch from tonic activity in juveniles to burst firing in egg-laying adults**

385 We next wanted to determine if the HSNs show activity as they develop and how
386 that activity compares to that seen in egg-laying adults. To follow HSN activity, we
387 expressed the Ca^{2+} reporter GCaMP5 along with mCherry in HSN using the *nlp-3*
388 promoter and performed ratiometric Ca^{2+} imaging as previously described (Collins et al.,
389 2016). Starting at the L4.7-8 larval stage, we observed rhythmic Ca^{2+} activity in both HSN
390 presynaptic termini and in the soma (Fig. 2A and 2B). During the L4.9 larval stage, when
391 animals exhibited behavioral features of the developmentally timed L4 quiescence
392 (Raizen et al., 2008), rhythmic Ca^{2+} activity in the HSNs slowed (Fig. 2B; Movie 1). In
393 adult animals, HSNs showed only infrequent activity in between bouts of egg laying, but
394 HSN activity switched to burst firing as animals entered the active state (Fig. 2B; Movie
395 2). We quantitated changes in HSN Ca^{2+} transient peak amplitude and frequency during
396 the different developmental stages and behavior states. We found no significant
397 differences in HSN Ca^{2+} transient amplitude (Fig. 2C), but we did observe significant
398 changes in frequency. The median inter-transient interval in L4.7-8 animals was ~34 s,
399 and this interval increased to ~60 s as animals reached the L4.9 stage (Fig. 2D). The
400 reduction of HSN transient frequency seen in L4.9 animals resembled the egg-laying
401 inactive state. However, none of the developmental stages recapitulated the 'burst' Ca^{2+}
402 activity with <20 s inter-transient intervals seen during the egg-laying active state (Fig.
403 2D). Together, these results indicate that the HSNs show tonic Ca^{2+} activity once their

404 morphological development is complete. HSN activity then switches into distinct inactive
405 and active states as animals become egg-laying adults.

406 The onset of Ca^{2+} activity in the HSN neurons during the late L4 stage coincided
407 with changes in animal locomotion, pharyngeal pumping, and defecation behaviors that
408 accompany the L4 lethargus (Raizen et al., 2008). Tonic HSN Ca^{2+} activity observed
409 during late L4 was suppressed after the completion of the molt. In adults, serotonin
410 release from the HSNs onto the AVF interneurons in the nerve ring has been shown to
411 increase locomotor arousal during the egg-laying active state (Hardaker et al., 2001). We
412 found that the frequency of HSN transients decreased as L4.9 animals enter lethargus,
413 consistent with a reduction in overall arousal and locomotion behavior. The ~50 s rhythm
414 of HSN activity in L4.9 animals resembles the defecation rhythm, prompting us to
415 investigate whether there is a relationship between HSN activity and the defecation motor
416 program (DMP). We found that defecation intervals in L4.7-8 and adult animals were
417 significantly longer when they were accompanied by one or more HSN Ca^{2+} transients
418 (Fig. 3A and 3B). HSNs make and receive synapses from the excitatory GABAergic AVL
419 motoneuron that regulates defecation, and serotonin and $G\alpha_o$ signaling have previously
420 been shown to inhibit defecation behavior (White et al., 1986; Segalat et al., 1995).
421 However, we found that optogenetic activation of the HSN neurons did not affect the
422 defecation rhythm in L4 or adult animals (Fig. 3C). Two independent mutants lacking
423 HSNs showed a significant decrease in DMP frequency (Fig. 3D), although this defecation
424 phenotype was not observed in *egl-47(dm)* animals which also reduce HSN
425 neurotransmitter release (Moresco and Koelle, 2004). The egg-laying and defecation
426 circuits both drive expulsion behaviors and are regulated by a common set of signaling

427 molecules (Reiner and Thomas, 1995), but a role for HSN in coordinating these behaviors
428 will require further study.

429 **Vulval muscles Ca^{2+} transients increase in strength and frequency during**
430 **development**

431 Since HSN promotes vulval muscle activity and egg laying in adults, we wanted to
432 determine if the HSN activity we observe in L4.7-8 and L4.9 animals drives early vulval
433 muscle activity. We used the *ceh-24* promoter to drive expression of GCaMP5 and
434 mCherry in the vulval muscles of L4 animals. We detected Ca^{2+} transients in the vulval
435 muscles at the L4.7-8 larval stage (Fig. 4A; Movie 3), and these transients continued in
436 L4.9 animals at increased frequency (Fig. 4B, 4C, 4F and 4G; Movies 4 and 5). The
437 median interval between vulval muscle Ca^{2+} transients was ~32 s in L4.7-8 animals which
438 dropped to 18 s in L4.9 animals. We compared juvenile activity to that seen in adults (Fig.
439 4D and 4E; Movie 6). Distributions of L4.9 Ca^{2+} transients were not significantly different
440 from vulval muscle twitch transients seen in adults during the egg-laying inactive state
441 (Fig. 4G). In contrast, the frequency of vulval muscle Ca^{2+} transients increased
442 significantly in animals during the egg-laying active state with median intervals dropping
443 to ~7 s phased with each body bend (Fig. 4G). We found that vulval muscle Ca^{2+}
444 transients also become stronger during development. While Ca^{2+} transient amplitudes in
445 the L4.7-8 and L4.9 stages were not significantly different, inactive phase Ca^{2+} transients
446 of adults were stronger than those observed in L4 animals (Fig. 4H). In adult animals,
447 strong Ca^{2+} transients were observed during the egg-laying active states, with the
448 strongest Ca^{2+} transients driving the complete and simultaneous contraction of anterior
449 and posterior vulval muscles to allow egg release (Fig. 4E and H).

450 We were surprised that vulval muscle transient frequencies decreased in adults as
451 circuit activity bifurcated into distinct inactive and active egg-laying behavior states. Based
452 on previous studies, we quantified periods of increased activity by measuring time spent
453 with vulval muscle Ca^{2+} transient intervals less than one minute (Collins and Koelle,
454 2013). We found that vulval muscle activity increased as L4.7-8 animals developed into
455 L4.9 animals but then dropped significantly in egg-laying adults. L4.7-8 animals on
456 average spent ~50% of their time in periods of increased vulval muscle activity, and this
457 increased to 85% as animals entered the L4.9 stage (Fig. 4I). In contrast, adult animals
458 spent only about ~33% of their time in periods with elevated vulval muscle activity (Fig.
459 4I) about half of which were coincident with the ~3 minute egg-laying active states that
460 occur about every 20 minutes (Waggoner et al., 1998). What depresses vulval muscle
461 activity in adult animals? We have previously shown that the loss of *unc-103*, which
462 encodes Ether-a-Go-Go Related Gene (ERG) K^+ channel, results in increased vulval
463 muscle excitability and egg-laying behavior (Collins and Koelle, 2013). Using an mCherry
464 transcriptional reporter transgene, we found that *unc-103e* expression in vulval muscles
465 is low in L4 animals and increases >15-fold as animals mature into egg-laying adults (Fig.
466 5). These results are consistent with our previous functional results that show that ERG
467 depresses vulval muscle electrical excitability in adults to promote distinct inactive and
468 active egg-laying behavior states (Collins and Koelle, 2013).

469 **Development of coordinated vulval muscle activity for egg laying**

470 Egg release through the vulva requires the synchronous contraction of the anterior
471 (A) and posterior (P) vulval muscles (Fig. 4E). Previous work has shown that loss of Notch
472 signaling blocks postsynaptic vm2 muscle arm development in L4 animals resulting in

473 asynchronous vulval muscle contractility and defects in egg-release in adults (Li et al.,
474 2013). Because of the vulval slit, the lateral vm2 muscle arms that develop between L4.7-
475 8 and L4.9 form the only sites of potential contact between the anterior and posterior
476 vulval muscles (Fig. 1M and 1N) (Li et al., 2013; Collins et al., 2016). To determine the
477 relationship between vulval muscle morphology and activity, we examined the spatial
478 distribution of vulval muscle Ca^{2+} during identified transients. We found that only 5% of
479 vulval muscle Ca^{2+} transients were coordinated in the L4.7-8 stage (Fig. 4A; Movie 3),
480 with nearly all transients occurring in either the anterior or posterior muscles (Fig. 4F and
481 4J). The degree of vulval muscle coordination increased significantly to ~28% of
482 transients during L4.9 (Fig. 4J; compare Movies 4 and 5) a time when vm1 and vm2
483 muscles, as well as vm2 muscle arms, complete their development (compare Fig. 1M and
484 1N). This level of coordinated muscle activity was not significantly different to that found
485 in adult animals during the egg-laying inactive state (Fig. 4J; compare Fig. 4C and 4D).
486 During the egg-laying active state ~60% of vulval muscle transients were found to be
487 coordinated, with Ca^{2+} transients occurring synchronously in the anterior and posterior
488 muscles (Movie 6). To test whether HSN activity was required for the development of
489 coordinated muscle activity, we analyzed muscle activity in animals missing the HSNs.
490 Surprisingly, we observed that vulval muscles develop wild-type levels of coordinated
491 activity even without HSN input (Fig. 4J). We have previously shown that vulval muscle
492 activity is phased with locomotion, possibly via rhythmic ACh release from the VA7 and
493 VB6 motor neurons onto the vm1 muscles (Collins et al., 2016). Our results suggest that
494 coordination of vulval muscle activity that develops by the L4.9 stage, is independent of

495 HSN input and may instead be a consequence of A/P muscle contact along the vulval slit
496 and driven by input from the locomotion central pattern generator.

497 **Early neuronal and vulval muscle activity is not required for the onset of adult egg-**
498 **laying behavior**

499 Activity in developing circuits has previously been shown to contribute to mature
500 patterns of activity that drive behavior. Is the activity we observe in HSN and vulval
501 muscles required for the proper onset of egg-laying behavior in adults? To test this, we
502 first set out to determine when adults initiate egg laying. Wild-type animals laid their first
503 egg at about ~6-7 hours after the L4-adult molt (Fig. 6A), a time when we first observed
504 VC and uv1 Ca^{2+} activity (data not shown). At this stage, animals had typically
505 accumulated ~8-10 eggs in the uterus. Animals without HSNs laid their first egg much
506 later, ~18 hours post molt (Fig. 6A). Gain-of-function receptor mutations in EGL-6, a
507 neuropeptide receptor coupled to $G\alpha_o$, or EGL-47*,* a putative gustatory receptor, block
508 neurotransmitter release from HSN, delaying egg release until ~15-17 hours after the L4
509 molt (Fig. 6A), resembling animals without HSNs (Moresco and Koelle, 2004; Ringstad
510 and Horvitz, 2008). Surprisingly, tryptophan hydroxylase *(tph-1*) knockout animals that
511 are unable to synthesize serotonin showed only a small albeit significant delay in egg
512 release compared to wild type (~7-8 hours post L4 molt), suggesting that HSN promotes
513 egg laying via release of neurotransmitters other than serotonin.

514 To silence HSN and vulval muscle activity acutely and reversibly, we expressed
515 *Drosophila* Histamine-gated chloride channels (HisCl) using cell-specific promoters and
516 tested how histamine affected egg-laying behavior (Pokala et al., 2014). Egg laying was

517 unaffected by exogenous histamine in non-transgenic animals but was potently inhibited
518 when HisCl channels were transgenically expressed in the HSNs, the vulval muscles, or
519 in the entire nervous system (Fig. 6B). Silencing these cells in late L4 animals for the
520 entire period where we observe early activity caused no significant changes in the onset
521 of adult egg laying after histamine washout in molted adults (Fig. 6C). We also observed
522 no change in the steady-state number of unlaid eggs in the uterus after developmental
523 silencing of L4 animals with histamine (data not shown). These results suggest that
524 presynaptic and postsynaptic activity in the developing circuit is not required for circuit
525 development or behavior.

526 **Vulval muscle responsiveness to HSN activity increases as maturing animals**
527 **accumulate unlaid eggs**

528 We have previously shown that optogenetic activation of the HSNs in adult animals
529 is sufficient to induce egg-laying circuit activity and behavior (Collins et al., 2016). Despite
530 the fact that both the HSNs and vulval muscles show activity in L4.9 animals, egg laying
531 does not begin until 6-7 hours later when the animals have accumulated ~8-10 unlaid
532 eggs in the uterus. In order to dissect the relationship between egg production,
533 developmental stage, and circuit activity, we tested when the vulval muscles develop
534 sensitivity to HSN input. We optogenetically activated the HSNs using Channelrhodopsin-
535 2 (ChR2) while simultaneously recording Ca^{2+} activity in the vulval muscles at 3 stages:
536 in L4.9 juveniles and in 3.5 hour and 6.5-hour old adults. L4.9 animals have no eggs in
537 the uterus, 3.5-hour adults contained 0-1 unlaid eggs, while 6.5-hour old adults had
538 accumulated ~8-10 eggs. Stimulating HSNs in L4.9 juveniles or in 3.5-hour adults failed
539 to induce detectable changes in vulval muscle Ca^{2+} activity (Fig. 7A, 7B, 7F). In contrast,

540 optogenetic activation of HSNs in 6.5-hour adults significantly increased vulval muscle
541 Ca^{2+} activity and triggered egg laying (Fig. 7C and 7F). L4.9 juveniles or 3.5-hour adults
542 with 0-1 eggs in the uterus had a mean transient frequency of ≤100 mHz, similar to the
543 inactive state vulval muscle Ca^{2+} response seen in 6.5-hour adult animals with ~8 unlaid
544 eggs grown in the absence of ATR, a cofactor necessary for ChR2 activation. The vulval
545 muscle Ca^{2+} response to HSN input was increased to ~170 mHz in 6.5-hour adults that
546 had accumulated ~8 unlaid eggs (Fig. 7G). The vulval muscles in serotonin-deficient
547 mutants responded normally to HSN activation at 6.5 hours (Fig. 7D and 7E), consistent
548 with the normal onset of egg laying in these mutants (Fig. 6A). Together, these results
549 show that despite having significant Ca^{2+} activity in juveniles, the adult vulval muscles
550 only develop a robust response to HSN input ~6 hours after the molt, a time when fertilized
551 embryos are being deposited in the uterus to be laid.

552 We next examined whether this change in vulval response in older adults was
553 caused by ongoing developmental events or was instead a consequence of egg
554 accumulation. We previously demonstrated that adults sterilized with FUDR, a chemical
555 blocker of germline cell division and egg production, showed inactive state levels of vulval
556 muscle activity (Collins et al., 2016). We found that vulval muscles in FUDR-treated
557 animals 24 hours after the molt were significantly less responsive to HSN optogenetic
558 stimulation (Fig. 8A and 8B). The residual vulval muscle response in FUDR-treated
559 animals is likely caused by incomplete sterilization when FUDR is added to L4.9 animals.
560 We interpret these results as indicating that egg accumulation, not animal age or circuit
561 maturity, modulates the onset of the egg-laying active state.

562 **A retrograde signal of egg accumulation and vulval muscle activity drives**
563 **presynaptic HSN activity**

564 HSN activity can be inhibited by external sensory signals and feedback of egg
565 release (Ringstad and Horvitz, 2008; Emtage et al., 2012; Collins et al., 2016; Banerjee
566 et al., 2017), but the factors that promote HSN activity are not clear. We tested whether
567 egg accumulation promotes circuit activity through the presynaptic HSNs, the
568 postsynaptic vulval muscles, or both. We found that HSN Ca^{2+} activity, particularly the
569 burst firing activity associated with the active state, was dramatically reduced in FUDR-
570 treated animals (Fig. 9A). Although we did observe single HSN Ca^{2+} transients after
571 FUDR treatment, the intervals in between were prolonged, often minutes apart (Fig. 9C).
572 We quantified the total time spent by animals with HSN Ca^{2+} transient intervals <30 s
573 apart as a measure of HSN burst-firing seen in the active state. We found that while
574 untreated animals spent ~13% of their time with the HSNs showing high-frequency
575 activity, such bursts were eliminated in FUDR-treated animals (Fig. 9D). This result shows
576 that feedback of egg production or accumulation modulates the frequency of HSN activity.

577 We performed a reciprocal experiment to test how the accumulation of unlaid eggs
578 would affect presynaptic HSN activity. We have previously shown that passage of eggs
579 through the vulva mechanically activates the uv1 neuroendocrine cells which release
580 tyramine and neuropeptides that inhibit HSN activity and egg laying (Collins et al., 2016;
581 Banerjee et al., 2017). We hypothesized that prevention of egg release would block
582 inhibitory uv1 feedback and increase HSN activity. We expressed HisCl channels in the
583 vulval muscles and recorded HSN Ca^{2+} activity after silencing with exogenous histamine.
584 Surprisingly, we found that acute silencing of vulval muscles significantly reduced

585 presynaptic HSN Ca^{2+} activity, resembling FUDR treatment (Fig. 9B and 9C). While
586 untreated animals spent ~16% of recording time with high frequency HSN activity, this
587 was reduced to ~2% of the total recording time in histamine-treated animals (Fig. 9D).
588 These results indicate that postsynaptic vulval muscle activity is required for the burst
589 firing in the presynaptic HSN neurons that accompanies the egg-laying active state.

590 We next looked at how HSN Ca^{2+} activity recovers when histamine inhibition of the
591 vulval muscles and egg laying is reversed. As shown in Fig. 10A, adult animals were
592 treated with or without histamine for 3-4 hours and then moved to plates without histamine
593 for a 20-30 minutes recovery period. Presynaptic HSN Ca^{2+} activity was then recorded as
594 the animals resumed egg-laying behavior. The HSNs showed a rapid and dramatic
595 recovery of Ca^{2+} activity after histamine washout resulting in a prolonged active state with
596 increased HSN Ca^{2+} transient frequency and numerous egg-laying events (Fig. 10A and
597 10B). Washout animals spent ~40% of their recorded time with elevated HSN activity
598 compared to 15% of the total recorded time in untreated controls (Fig. 10C). During this
599 recovery period, we observed increased vulval muscle twitching contractions in the bright
600 field channel, indicating that muscle activity was restored (data not shown). These results
601 are consistent with a model whereby accumulation of unlaid eggs promotes vulval muscle
602 activity which drives a homeostatic increase in HSN activity and burst-firing that sustains
603 egg laying.

604 HSN synapses are formed exclusively on the vm2 muscle arms that provide sites
605 of contact between the anterior and posterior vulval muscles (White et al., 1986; Collins
606 and Koelle, 2013; Li et al., 2013). Hypomorphic Notch signaling mutants fail to develop
607 vm2 muscle arms, and are egg-laying defective, but have normal pre-synaptic HSN and

608 VC development (Sundaram and Greenwald, 1993; Li et al., 2013). To determine if
609 retrograde signaling from the vulval muscles to the HSNs occurs through the vm2 muscle
610 arms, we recorded HSN Ca^{2+} activity in *lin-12(wy750)* Notch receptor mutant animals
611 (Fig. 11A and 11B). We found that HSN Ca^{2+} transient frequency was strongly reduced
612 in the *lin-12(wy750)* mutants compared to wild-type control animals (Fig. 11C and 11D).
613 HSN Ca^{2+} transients still occurred in this mutant, but burst-firing was eliminated. Wild-
614 type animals spent ~13% of their time with HSN transients <30 s apart, while this was
615 zero in the *lin-12(wy750)* mutant (Fig. 11E), resembling activity seen in FUDR-sterilized
616 or vulval muscle-silenced animals. Together, these results suggest that muscle activity
617 feeds back through the vm2 muscle arms onto the pre-synaptic HSN neurons to promote
618 additional Ca^{2+} transients that drive burst firing and sustain the egg-laying active state.

619

620 **Discussion**

621 We used a combination of molecular genetic, optogenetic, and ratiometric Ca^{2+}
622 imaging approaches to determine how coordinated activity develops in the *C. elegans*
623 egg-laying behavior circuit. We find the pre-synaptic HSNs, VCs, and uv1 neuroendocrine
624 cells complete morphological development in the early-mid L4 stages, while the vulval
625 muscles finish developing at the late L4 stages. Like HSNs, the vulval muscles show Ca^{2+}
626 activity in the L4.7-8 stage. Coordinated vulval muscle Ca^{2+} transients are not observed
627 until the L4.9 stage, a time when the anterior and posterior vm2 muscle arms complete a
628 Notch-dependent lateral extension around the primary vulval epithelial cells (Li et al.,
629 2013). We do not observe Ca^{2+} transients in the VC neurons and uv1 cells except in egg-

630 laying adults (data not shown) suggesting activity in these cells does not contribute to
631 circuit development. In adults, the juvenile HSN and vulval muscle activity disappears,
632 leading to the establishment of characteristic 'inactive' states in which adult animals
633 spend ~85% of their time. Inactive state activity closely resembles that seen in sterilized
634 animals that do not accumulate any eggs. Figure 12 shows a working model for how
635 postsynaptic muscle activity could promote burst firing in the presynaptic HSNs. We
636 propose that uterine cells depress or excite the vulval muscles depending on the degree
637 of stretch. Activation of the uterine muscles, which make gap junctions onto the vm2
638 muscles, would increase vulval muscle sensitivity to serotonin and other
639 neurotransmitters released from HSN, which subsequently allows for rhythmic ACh input
640 from the VA/VB locomotion motor neurons to drive vulval muscle twitching contractions.
641 Coordinated Ca^{2+} activity in the anterior and posterior vulval muscles diffuses into the
642 vm2 muscle arms to restimulate the HSNs and prolong the egg-laying active state. VC
643 activity is coincident with strong vulval muscle contractions, while uv1 activity follows
644 passage of eggs through the vulva. Signals released from one or more of these cells may
645 increase the short-term probability of subsequent HSN Ca^{2+} transients during a burst.
646 Once sufficient eggs have been laid, excitatory feedback into the vulval muscles and back
647 to the HSNs is reduced, increasing the probability that inhibitory ACh, tyramine, and
648 neuropeptides released from VC and uv1 will block subsequent HSN Ca^{2+} transients,
649 returning the circuit to the inactive state.

650 Changes in gene expression likely contribute to the changes in circuit activity
651 patterns we observe between L4s and adults. Previous work has found that serotonin
652 expression is low in L4 and increases as animals increase egg laying (Tanis et al., 2008).

653 Since mutants lacking serotonin have little effect on the timing of the first egg-laying event,
654 we anticipate other neurotransmitters released from the HSNs promote egg laying in
655 young adults. KCC-2 and ABTS-1, two Cl^- extruders required for inhibitory
656 neurotransmission, show a developmental increase in HSN expression from L4 to adult
657 (Tanis et al., 2009; Bellemer et al., 2011) which may be associated with the
658 disappearance of spontaneous rhythmic activity in the HSNs after the late L4 stages. At
659 the same time, we find that inhibitory ERG K^+ channel expression becomes upregulated
660 in the vulval muscles of young adults. Studies in vertebrate models have shown that
661 mechanical stretch can increase the transcription of receptors that enhance muscle
662 contraction during parturition (Terzidou et al., 2005; Shynlova et al., 2007). We speculate
663 that similar mechanisms may operate in the *C. elegans* reproductive system to drive
664 expression of receptors and channels that modulate vulval muscle sensitivity to
665 presynaptic input. Identifying additional genes whose expression increases upon egg
666 accumulation could help explain how HSN-deficient animals are still able to enter
667 otherwise normal egg-laying active states after sufficient eggs have accumulated.

668 The HSNs show dramatic changes in Ca^{2+} transient frequency between the
669 inactive and active states. Major G proteins, $G\alpha_q$ and $G\alpha_o$, signal in HSN to increase and
670 inhibit egg laying, respectively (Ringstad and Horvitz, 2008; Tanis et al., 2008). G protein
671 signaling in HSN may modulate an intrinsic pacemaker activity, similar to that seen in
672 other central pattern generator circuits and in the cardiac pacemaker (Hille, 2001). $G\alpha_o$
673 signaling in HSN activates inhibitory IRK K^+ channels (Emtage et al., 2012), and recent
674 work has identified the T-type Ca^{2+} channel, CCA-1, and the Na^+ leak channels, NCA-1
675 and NCA-2, as possible targets of excitatory $G\alpha_q$ signaling (Yeh et al., 2008; Topalidou

676 et al., 2012; Zang et al., 2017). The balance of both G protein signaling pathways would
677 allow for HSN frequency modulation and dictate whether animals enter or leave the egg-
678 laying active state.

679 Early vulval muscle activity may be spontaneous or driven by neuronal input.
680 Spontaneous Ca^{2+} transients promote the maturation of activity in many other cells
681 (Moody and Bosma, 2005). We observed no change in behavioral onset or egg-laying
682 rate in animals in which neuron or vulval muscle activity was silenced in the L4 stage.
683 While this may result from incomplete silencing using the HisCl based approach, previous
684 results in other circuits indicate synapse development does not require Ca^{2+}-dependent
685 excitatory transmission (Verhage et al., 2000; Lu et al., 2013; Sando et al., 2017). While
686 G protein signaling may drive early Ca^{2+} activity in the absence of electrical activity,
687 synaptic transmission would still require Ca^{2+}-dependent vesicle fusion. The persistence
688 of vulval muscle activity in animals that lack HSNs and its recovery after acute neural
689 silencing suggests the activity we observe arises from a shared mechanism that is not
690 strictly required for synapse development and/or recovers quickly after histamine
691 washout.

692 Our work continues to show the functional importance of the post-synaptic vm2
693 muscle arms in coordinating muscle activity during egg-laying behavior. Because of the
694 intervening vulval slit through which eggs are laid, the vm2 muscle arms are the only sites
695 of contact between the anterior and posterior muscles. Coordinated muscle Ca^{2+}
696 transients appear during the L4.9 larval stage after vm2 muscle arm development. After
697 development, the vm2 muscle arms may be electrically coupled at their points of contact,
698 allowing for the immediate spread of electrical activity and/or Ca^{2+} signals between the

699 anterior and posterior muscles. In addition to uncoordinated vm1 and vm2 Ca^{2+} activity
700 (Li et al., 2013), these mutants do not show regenerative HSN Ca^{2+} activity, resembling
701 the consequences of vulval muscle electrical silencing. The vm2 muscle arms also form
702 the sites of synaptic input from HSN and VC. We have previously shown that the ERG K^+
703 channel and SER-1 serotonin receptor localize to the vm2 muscle arm region (Collins and
704 Koelle, 2013; Li et al., 2013). Both ERG and SER-1 have C-terminal PDZ interaction
705 motifs, and SER-1 has been shown to interact with the large PDZ scaffold protein MPZ-1
706 that may drive the local organization of these and other molecules to the vm2 muscle
707 arms (Xiao et al., 2006). Innexin gap junction proteins which are potential targets of G
708 protein signaling (Correa et al., 2015) may also play a role in driving the development of
709 coordinated vulval muscle contractility and HSN 'burst' activity in the circuit during egg
710 laying.

711 Neural circuits which generate directional movements during peristalsis, axial
712 locomotion, and swimming rely on central pattern generator (CPG) circuits which possess
713 intrinsic rhythms (Grillner, 2003). Sensory feedback as well as dedicated groups of
714 sensory interneurons regulate the spatio-temporal patterns of activation of motor neurons
715 controlled by CPG circuits (Marder et al., 2005; Miles and Sillar, 2011). In *Drosophila*, the
716 segmentally distributed GDL interneurons receive stretch sensory input and control the
717 rhythmic activation of motor neurons during larval locomotion (Fushiki et al., 2016). In
718 guinea-pigs, stretch-sensitive ascending and descending interneurons in the distal colon
719 provide rhythmic excitatory and inhibitory inputs to enteric motor neurons during
720 peristalsis (Spencer et al., 2006). The *C. elegans* egg-laying system also appears to

721 contain stretch-sensitive modalities, possibly relying on physiological mechanisms similar
722 to those described above (Li et al., 2006; Hu et al., 2011; Wen et al., 2012).

723 The VC motor neurons share key functional features of sensory neurons and
724 interneurons which modulate CPG rhythms in other circuits. VC extends non-synaptic
725 processes along the vulval hypodermis which could be mechanically activated by vulval
726 muscle contraction (White et al., 1986; Colavita and Tessier-Lavigne, 2003). The VC
727 neurons make synapses onto both the vm2 vulval muscles and the body wall muscles.
728 The VCs also make gap junctions with both the vm2 vulval muscles and the HSNs. VC
729 Ca^{2+} activity peaks at the moment of vulval muscle contraction, but optogenetic activation
730 of the VCs fails to elicit egg laying events and instead slows locomotion. Moreover, VC-
731 and acetylcholine-defective mutants show increased egg laying (Bany et al., 2003;
732 Ringstad and Horvitz, 2008), suggesting a loss of inhibitory feedback. Thus, the VCs,
733 instead of releasing acetylcholine at the vm2 synapse to drive vulval muscle contraction,
734 may function in part as baroreceptors to slow locomotion during egg release (Collins et
735 al., 2016). Our studies of the egg-laying circuit show that ongoing HSN activity depends
736 on a signal released from the post-synaptic vulval muscles induced by stretch-dependent
737 activation. Further studies of the egg-laying circuit should allow for the identification of the
738 molecules and cells that drive this unique form of retrograde modulation of presynaptic
739 activity.

740

741 **References:**

742 Adler CE, Fetter RD, Bargmann CI (2006) UNC-6/Netrin induces neuronal asymmetry
743 and defines the site of axon formation. Nat Neurosci 9:511-518.

744 Akerboom J et al. (2013) Genetically encoded calcium indicators for multi-color neural
745 activity imaging and combination with optogenetics. Front Mol Neurosci 6:2.

746 Banerjee N, Bhattacharya R, Gorczyca M, Collins KM, Francis MM (2017) Local
747 neuropeptide signaling modulates serotonergic transmission to shape the
748 temporal organization of *C. elegans* egg-laying behavior. PLoS Genet
749 13:e1006697.

750 Bany IA, Dong MQ, Koelle MR (2003) Genetic and cellular basis for acetylcholine
751 inhibition of *Caenorhabditis elegans* egg-laying behavior. J Neurosci 23:8060-
752 8069.

753 Bellemer A, Hirata T, Romero MF, Koelle MR (2011) Two types of chloride transporters
754 are required for GABA(A) receptor-mediated inhibition in *C. elegans*. EMBO J
755 30:1852-1863.

756 Borodinsky LN, Root CM, Cronin JA, Sann SB, Gu X, Spitzer NC (2004) Activity-
757 dependent homeostatic specification of transmitter expression in embryonic
758 neurons. Nature 429:523-530.

759 Brenner S (1974) The genetics of *Caenorhabditis elegans*. Genetics 77:71-94.

760 Cai T, Fukushige T, Notkins AL, Krause M (2004) Insulinoma-Associated Protein IA-2, a
761 Vesicle Transmembrane Protein, Genetically Interacts with UNC-31/CAPS and
762 Affects Neurosecretion in *Caenorhabditis elegans*. J Neurosci 24:3115-3124.

763 Carnell L, Illi J, Hong SW, McIntire SL (2005) The G-protein-coupled serotonin receptor
764 SER-1 regulates egg laying and male mating behaviors in *Caenorhabditis elegans*.
765 J Neurosci 25:10671-10681.
766 Chase DL, Pepper JS, Koelle MR (2004) Mechanism of extrasynaptic dopamine signaling
767 in *Caenorhabditis elegans*. Nat Neurosci 7:1096-1103.
768 Clark SG, Lu X, Horvitz HR (1994) The *Caenorhabditis elegans* locus lin-15, a negative
769 regulator of a tyrosine kinase signaling pathway, encodes two different proteins.
770 Genetics 137:987-997.
771 Colavita A, Tessier-Lavigne M (2003) A Neurexin-related protein, BAM-2, terminates
772 axonal branches in *C. elegans*. Science 302:293-296.
773 Collins KM, Koelle MR (2013) Postsynaptic ERG potassium channels limit muscle
774 excitability to allow distinct egg-laying behavior states in *Caenorhabditis elegans*.
775 J Neurosci 33:761-775.
776 Collins KM, Bode A, Fernandez RW, Tanis JE, Brewer JC, Creamer MS, Koelle MR
777 (2016) Activity of the *C. elegans* egg-laying behavior circuit is controlled by
778 competing activation and feedback inhibition. Elife 5:e21126.
779 Correa PA, Gruninger T, Garcia LR (2015) DOP-2 D2-Like Receptor Regulates UNC-7
780 Innexins to Attenuate Recurrent Sensory Motor Neurons during *C. elegans*
781 Copulation. J Neurosci 35:9990-10004.
782 Dempsey CM, Mackenzie SM, Gargus A, Blanco G, Sze JY (2005) Serotonin (5HT),
783 fluoxetine, imipramine and dopamine target distinct 5HT receptor signaling to
784 modulate *Caenorhabditis elegans* egg-laying behavior. Genetics 169:1425-1436.

785 Dernovici S, Starc T, Dent JA, Ribeiro P (2007) The serotonin receptor SER-1 (5HT2ce)
786 contributes to the regulation of locomotion in *Caenorhabditis elegans*. Dev
787 Neurobiol 67:189-204.
788 Emtage L, Aziz-Zaman S, Padovan-Merhar O, Horvitz HR, Fang-Yen C, Ringstad N
789 (2012) IRK-1 potassium channels mediate peptidergic inhibition of *Caenorhabditis*
790 *elegans* serotonin neurons via a G(o) signaling pathway. J Neurosci 32:16285-
791 16295.
792 Flavell SW, Pokala N, Macosko EZ, Albrecht DR, Larsch J, Bargmann CI (2013)
793 Serotonin and the neuropeptide PDF initiate and extend opposing behavioral
794 states in *C. elegans*. Cell 154:1023-1035.
795 Fushiki A, Zwart MF, Kohsaka H, Fetter RD, Cardona A, Nose A (2016) A circuit
796 mechanism for the propagation of waves of muscle contraction in *Drosophila*. Elife
797 5:13253.
798 Garaschuk O, Hanse E, Konnerth A (1998) Developmental profile and synaptic origin of
799 early network oscillations in the CA1 region of rat neonatal hippocampus. J Physiol
800 507 (Pt 1):219-236.
801 Garaschuk O, Linn J, Eilers J, Konnerth A (2000) Large-scale oscillatory calcium waves
802 in the immature cortex. Nat Neurosci 3:452-459.
803 Grillner S (2003) The motor infrastructure: from ion channels to neuronal networks. Nat
804 Rev Neurosci 4:573-586.
805 Gu X, Spitzer NC (1995) Distinct aspects of neuronal differentiation encoded by frequency
806 of spontaneous Ca^{2+} transients. Nature 375:784-787.

807 Gu X, Olson EC, Spitzer NC (1994) Spontaneous neuronal calcium spikes and waves
808 during early differentiation. J Neurosci 14:6325-6335.
809 Gurel G, Gustafson MA, Pepper JS, Horvitz HR, Koelle MR (2012) Receptors and other
810 signaling proteins required for serotonin control of locomotion in *Caenorhabditis*
811 *elegans*. Genetics 192:1359-1371.
812 Hanson MG, Milner LD, Landmesser LT (2008) Spontaneous rhythmic activity in early
813 chick spinal cord influences distinct motor axon pathfinding decisions. Brain Res
814 Rev 57:77-85.
815 Hapiak VM, Hobson RJ, Hughes L, Smith K, Harris G, Condon C, Komuniecki P,
816 Komuniecki RW (2009) Dual excitatory and inhibitory serotonergic inputs modulate
817 egg laying in *Caenorhabditis elegans*. Genetics 181:153-163.
818 Hardaker LA, Singer E, Kerr R, Zhou G, Schafer WR (2001) Serotonin modulates
819 locomotory behavior and coordinates egg-laying and movement in *Caenorhabditis*
820 *elegans*. J Neurobiol 49:303-313.
821 Harfe BD, Fire A (1998) Muscle and nerve-specific regulation of a novel NK-2 class
822 homeodomain factor in *Caenorhabditis elegans*. Development 125:421-429.
823 Hille B (2001) Ion Channels of Excitable Membranes, Third Edition: Sinaur.
824 Hobson RJ, Hapiak VM, Xiao H, Buehrer KL, Komuniecki PR, Komuniecki RW (2006)
825 SER-7, a *Caenorhabditis elegans* 5-HT7-like receptor, is essential for the 5-HT
826 stimulation of pharyngeal pumping and egg laying. Genetics 172:159-169.
827 Hu Z, Pym EC, Babu K, Vashlishan Murray AB, Kaplan JM (2011) A neuropeptide-
828 mediated stretch response links muscle contraction to changes in neurotransmitter
829 release. Neuron 71:92-102.

830 Jarecki J, Keshishian H (1995) Role of neural activity during synaptogenesis in
831 *Drosophila*. J Neurosci 15:8177-8190.
832 Li C, Chalfie M (1990) Organogenesis in *C. elegans*: positioning of neurons and muscles
833 in the egg-laying system. Neuron 4:681-695.
834 Li P, Collins KM, Koelle MR, Shen K (2013) LIN-12/Notch signaling instructs postsynaptic
835 muscle arm development by regulating UNC-40/DCC and MADD-2 in
836 *Caenorhabditis elegans*. Elife 2:e00378.
837 Li W, Feng Z, Sternberg PW, Xu XZ (2006) A *C. elegans* stretch receptor neuron revealed
838 by a mechanosensitive TRP channel homologue. Nature 440:684-687.
839 Lu W, Bushong EA, Shih TP, Ellisman MH, Nicoll RA (2013) The cell-autonomous role of
840 excitatory synaptic transmission in the regulation of neuronal structure and
841 function. Neuron 78:433-439.
842 Marder E, Bucher D, Schulz DJ, Taylor AL (2005) Invertebrate central pattern generation
843 moves along. Curr Biol 15:R685-699.
844 Miles GB, Sillar KT (2011) Neuromodulation of vertebrate locomotor control networks.
845 Physiology (Bethesda) 26:393-411.
846 Mok DZ, Sternberg PW, Inoue T (2015) Morphologically defined sub-stages of *C. elegans*
847 vulval development in the fourth larval stage. BMC Dev Biol 15:26.
848 Moody WJ, Bosma MM (2005) Ion channel development, spontaneous activity, and
849 activity-dependent development in nerve and muscle cells. Physiol Rev 85:883-
850 941.

851 Moresco JJ, Koelle MR (2004) Activation of EGL-47, a Galpha(o)-coupled receptor,
852 inhibits function of hermaphrodite-specific motor neurons to regulate
853 *Caenorhabditis elegans* egg-laying behavior. J Neurosci 24:8522-8530.
854 Patel MR, Lehrman EK, Poon VY, Crump JG, Zhen M, Bargmann CI, Shen K (2006)
855 Hierarchical assembly of presynaptic components in defined *C. elegans* synapses.
856 Nat Neurosci 9:1488-1498.
857 Pokala N, Liu Q, Gordus A, Bargmann CI (2014) Inducible and titratable silencing of
858 *Caenorhabditis elegans* neurons in vivo with histamine-gated chloride channels.
859 Proc Natl Acad Sci U S A 111:2770-2775.
860 Raizen DM, Zimmerman JE, Maycock MH, Ta UD, You YJ, Sundaram MV, Pack AI (2008)
861 Lethargus is a *Caenorhabditis elegans* sleep-like state. Nature 451:569-572.
862 Ravi B, Nassar LM, Kopchock RJ, Dhakal P, Collins KM (2018) Ratiometric Calcium
863 Imaging of Individual Neurons in Behaving *Caenorhabditis elegans* (in press).
864 Journal of Visualized Experiments.
865 Reiner DJ, Thomas JH (1995) Reversal of a muscle response to GABA during *C. elegans*
866 male development. J Neurosci 15:6094-6102.
867 Ringstad N, Horvitz HR (2008) FMRFamide neuropeptides and acetylcholine
868 synergistically inhibit egg-laying by *C. elegans*. Nat Neurosci 11:1168-1176.
869 Sando R, Bushong E, Zhu Y, Huang M, Considine C, Phan S, Ju S, Uytiepo M, Ellisman
870 M, Maximov A (2017) Assembly of Excitatory Synapses in the Absence of
871 Glutamatergic Neurotransmission. Neuron 94:312-321 e313.
872 Schafer WR, Sanchez BM, Kenyon CJ (1996) Genes affecting sensitivity to serotonin in
873 *Caenorhabditis elegans*. Genetics 143:1219-1230.

874 Segalat L, Elkes DA, Kaplan JM (1995) Modulation of serotonin-controlled behaviors by
875 Go in *Caenorhabditis elegans*. Science 267:1648-1651.
876 Shen K, Bargmann CI (2003) The immunoglobulin superfamily protein SYG-1 determines
877 the location of specific synapses in *C. elegans*. Cell 112:619-630.
878 Shen K, Fetter RD, Bargmann CI (2004) Synaptic specificity is generated by the synaptic
879 guidepost protein SYG-2 and its receptor, SYG-1. Cell 116:869-881.
880 Shynlova O, Williams SJ, Draper H, White BG, MacPhee DJ, Lye SJ (2007) Uterine
881 stretch regulates temporal and spatial expression of fibronectin protein and its
882 alpha 5 integrin receptor in myometrium of unilaterally pregnant rats. Biol Reprod
883 77:880-888.
884 Spencer NJ, Dickson EJ, Hennig GW, Smith TK (2006) Sensory elements within the
885 circular muscle are essential for mechanotransduction of ongoing peristaltic reflex
886 activity in guinea-pig distal colon. J Physiol 576:519-531.
887 Sundaram M, Greenwald I (1993) Suppressors of a lin-12 hypomorph define genes that
888 interact with both lin-12 and glp-1 in *Caenorhabditis elegans*. Genetics 135:765-
889 783.
890 Tanis JE, Moresco JJ, Lindquist RA, Koelle MR (2008) Regulation of serotonin
891 biosynthesis by the G proteins Galphao and Galphaq controls serotonin signaling
892 in *Caenorhabditis elegans*. Genetics 178:157-169.
893 Tanis JE, Bellemer A, Moresco JJ, Forbush B, Koelle MR (2009) The potassium chloride
894 cotransporter KCC-2 coordinates development of inhibitory neurotransmission and
895 synapse structure in *Caenorhabditis elegans*. J Neurosci 29:9943-9954.

896 Terzidou V, Sooranna SR, Kim LU, Thornton S, Bennett PR, Johnson MR (2005)
897 Mechanical stretch up-regulates the human oxytocin receptor in primary human
898 uterine myocytes. J Clin Endocrinol Metab 90:237-246.
899 Thomas JH (1990) Genetic analysis of defecation in Caenorhabditis elegans. Genetics
900 124:855-872.
901 Topalidou I, Keller C, Kalebic N, Nguyen KC, Somhegyi H, Politi KA, Heppenstall P, Hall
902 DH, Chalfie M (2012) Genetically separable functions of the MEC-17 tubulin
903 acetyltransferase affect microtubule organization. Curr Biol 22:1057-1065.
904 Tsalik EL, Hobert O (2003) Functional mapping of neurons that control locomotory
905 behavior in *Caenorhabditis elegans*. J Neurobiol 56:178-197.
906 Verhage M, Maia AS, Plomp JJ, Brussaard AB, Heeroma JH, Vermeer H, Toonen RF,
907 Hammer RE, van den Berg TK, Missler M, Geuze HJ, Sudhof TC (2000) Synaptic
908 assembly of the brain in the absence of neurotransmitter secretion. Science
909 287:864-869.
910 Waggoner LE, Zhou GT, Schafer RW, Schafer WR (1998) Control of alternative
911 behavioral states by serotonin in Caenorhabditis elegans. Neuron 21:203-214.
912 Warp E, Agarwal G, Wyart C, Friedmann D, Oldfield CS, Conner A, Del Bene F, Arrenberg
913 AB, Baier H, Isacoff EY (2012) Emergence of patterned activity in the developing
914 zebrafish spinal cord. Curr Biol 22:93-102.
915 Watt AJ, Cuntz H, Mori M, Nusser Z, Sjostrom PJ, Hausser M (2009) Traveling waves in
916 developing cerebellar cortex mediated by asymmetrical Purkinje cell connectivity.
917 Nat Neurosci 12:463-473.

918 Wen Q, Po MD, Hulme E, Chen S, Liu X, Kwok SW, Gershow M, Leifer AM, Butler V,
919 Fang-Yen C, Kawano T, Schafer WR, Whitesides G, Wyart M, Chklovskii DB, Zhen
920 M, Samuel AD (2012) Proprioceptive coupling within motor neurons drives *C.*
921 *elegans* forward locomotion. Neuron 76:750-761.
922 White JG, Southgate E, Thomson JN, Brenner S (1986) The structure of the nervous
923 system of the nematode *Caenorhabditis elegans*. Philos Trans R Soc Lond B Biol
924 Sci 314:1-340.
925 Wong RO, Chernjavsky A, Smith SJ, Shatz CJ (1995) Early functional neural networks in
926 the developing retina. Nature 374:716-718.
927 Xiao H, Hapiak VM, Smith KA, Lin L, Hobson RJ, Plenefisch J, Komuniecki R (2006) SER-
928 1, a *Caenorhabditis elegans* 5-HT2-like receptor, and a multi-PDZ domain
929 containing protein (MPZ-1) interact in vulval muscle to facilitate serotonin-
930 stimulated egg-laying. Dev Biol 298:379-391.
931 Yeh E, Ng S, Zhang M, Bouhours M, Wang Y, Wang M, Hung W, Aoyagi K, Melnik-
932 Martinez K, Li M, Liu F, Schafer WR, Zhen M (2008) A putative cation channel,
933 NCA-1, and a novel protein, UNC-80, transmit neuronal activity in *C. elegans*.
934 PLoS Biol 6:e55.
935 Zang KE, Ho E, Ringstad N (2017) Inhibitory peptidergic modulation of *C. elegans*
936 serotonin neurons is gated by T-type calcium channels. Elife 6:e22771.

937

938

939

940 **Figures**

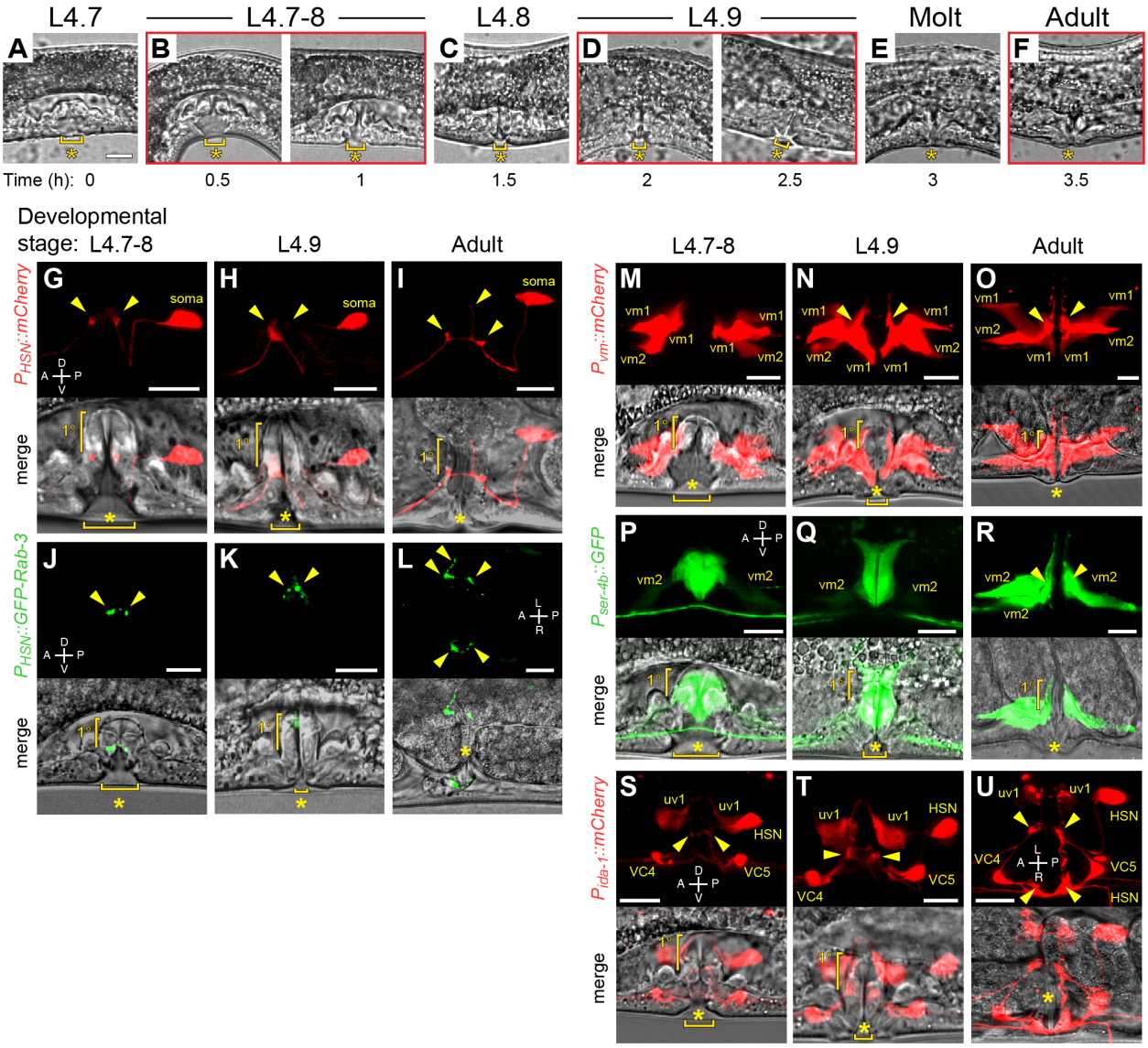

941

942 **Fig. 1: Morphological development of the *C. elegans* egg-laying circuit**. (A-F)
943 Representative images of vulval morphology at late L4 stages- (A) L4.7, (B) L4.7-8, (C)
944 L4.8, (D) L4.9, (E) Molt and (F) Young adult. (G-I) Morphology of HSN (top) and vulva
945 (bottom) in L4.7-8 (G) and L4.9 (H) larval stages and in adults (I). (J-L) Morphology of
946 HSN synapses (top) and vulva (bottom) in L4.7-8 (J) and L4.9 (K) larval stages and in

947 adults (L). Arrowheads indicate RAB-3-GFP presynaptic puncta. (M-O) Morphology of
948 vm1 and vm2 vulval muscles (top) and vulva (bottom) in L4.7-8 (M) and L4.9 (N) larval
949 stages and in adults (O). (P-R) Developmental expression of *ser-4* from a GFP
950 transcriptional reporter at the L4.7-8 (P) and L4.9 (Q) larval stages and in adults (R). (S-
951 U) Morphology of HSN, VC4, VC5, and the uv1 neuroendocrine cells (top) and vulva
952 (bottom) in L4.7-8 (S) and L4.9 (T) larval stages and in adults (U) visualized using the
953 *ida-1* promoter. Arrowheads in all images indicate the location of presynaptic boutons or
954 postsynaptic vm2 muscle arms. Scale bar is 10 μm, and asterisk indicates the position of
955 the developing or completed vulval opening. Vertical half-brackets indicate the
956 approximate position of primary (1°) vulval epithelial cells, and horizontal bracket
957 indicates progress of vulval lumen collapse at each larval stage.
958

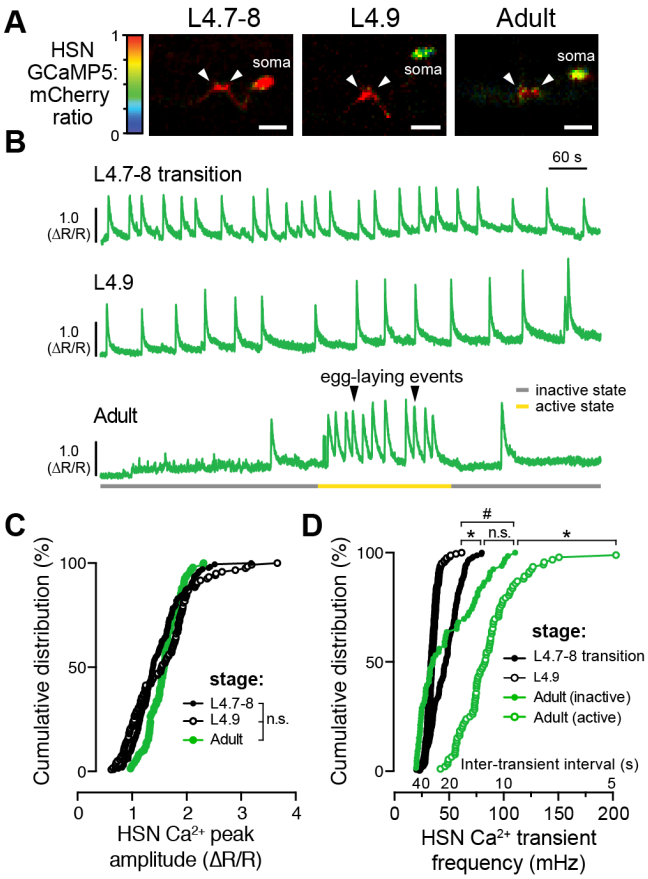

Fig. 2. HSN neurons show tonic Ca^{2+} activity during the late L4 stage and burst firing during the egg-laying active state. (A) Micrographs of the intensity-modulated GCaMP5:mCherry fluorescence ratio during HSN Ca^{2+} transients in L4.7-8 and L4.9 larval stages, and in adults. White arrowheads show Ca^{2+} activity localized to the anterior and posterior presynaptic boutons. Scale bar is 10μm; anterior is at left, ventral is at bottom. See also Movies S1 and S2. (B) Representative GCaMP5:mCherry ratio traces (ΔR/R) of HSN Ca^{2+} activity in L4.7-8 (top), L4.9 (middle), and in adult animals (bottom). Adults show distinct active (yellow) and inactive (grey) egg-laying behavior states. Black arrowheads indicate egg-laying events. (C) Cumulative distributions of HSN Ca^{2+} peak amplitudes in L4.7-8 (closed black circles), L4.9 (open black circles), and adults (closed green circles). n.s. indicates p>0.0809 (one-way ANOVA). (D) Cumulative distribution

971 plots of instantaneous HSN Ca^{2+} transient frequencies (and inter-transient intervals) from
972 L4.7-8 (closed black circles) and L4.9 (open black circles) animals, and from adult egg-
973 laying inactive (green closed circles) and active (green open circles) states. Asterisks (*)
974 indicate $p<0.0001$; pound sign (#) indicates $p=0.0283$; n.s. indicates $p=0.1831$ (Kruskal-
975 Wallis test).

976

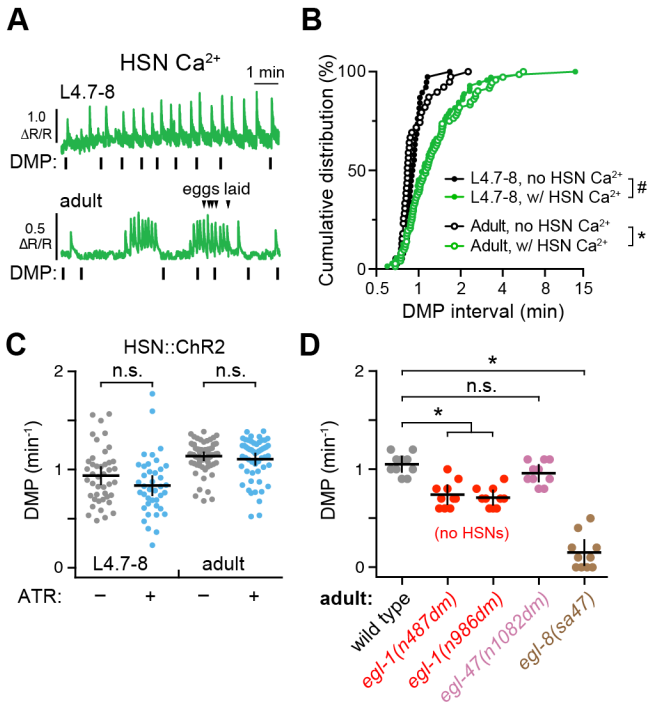

977

978 **Fig. 3: HSN regulates the defecation motor program.** (A) Representative HSN Ca^{2+}
979 traces at the L4.7-8 larval stage (top) and adults (bottom). Vertical lines indicate the
980 expulsion step of the defecation motor program (DMP); arrowheads indicate adult egg-
981 laying events. (B) Cumulative distribution plots showing DMP intervals with no HSN Ca^{2+}
982 transient (black) versus those with one or more HSN Ca^{2+} transients (green) in L4.7-8
983 (closed circles) and adult (open circles). Pound indicates p=0.0058; asterisk indicates
984 p<0.0001 (Kruskal-Wallis test with Dunn's correction for multiple comparisons). (C)
985 Scatter plots showing the consequences of HSN optogenetic activation on the DMP
986 Expulsion step frequency. L4.7-8 and adult animals expressing Channelrhodpsin-2 in
987 HSN neurons were grown in the absence (-, grey) or presence (+, blue) of all-*trans* retinal
988 (ATR), illuminated with blue light for two minutes, and the timing of DMP events was used
989 to calculate an instantaneous DMP frequency. Error bars show 95% confidence intervals
990 for the mean; n.s. indicates p=0.0645 (L4.7-8) or p=0.1866, (adult) (Student's t test). (D)

991 Scatter plots showing DMP frequencies (min^{-1}) in wild-type (grey), *egl-1(n487dm)* and
992 *egl-1(n986dm)* (red), *egl-47(n1082dm)* (pink), and *egl-8(sa47)* (brown) adults. Error bars
993 indicate the 95% confidence interval for the mean. Asterisk indicates $p<0.0001$; n.s.
994 indicates $p=0.5208$ (One-way ANOVA with Bonferroni's correction for multiple
995 comparisons).
996

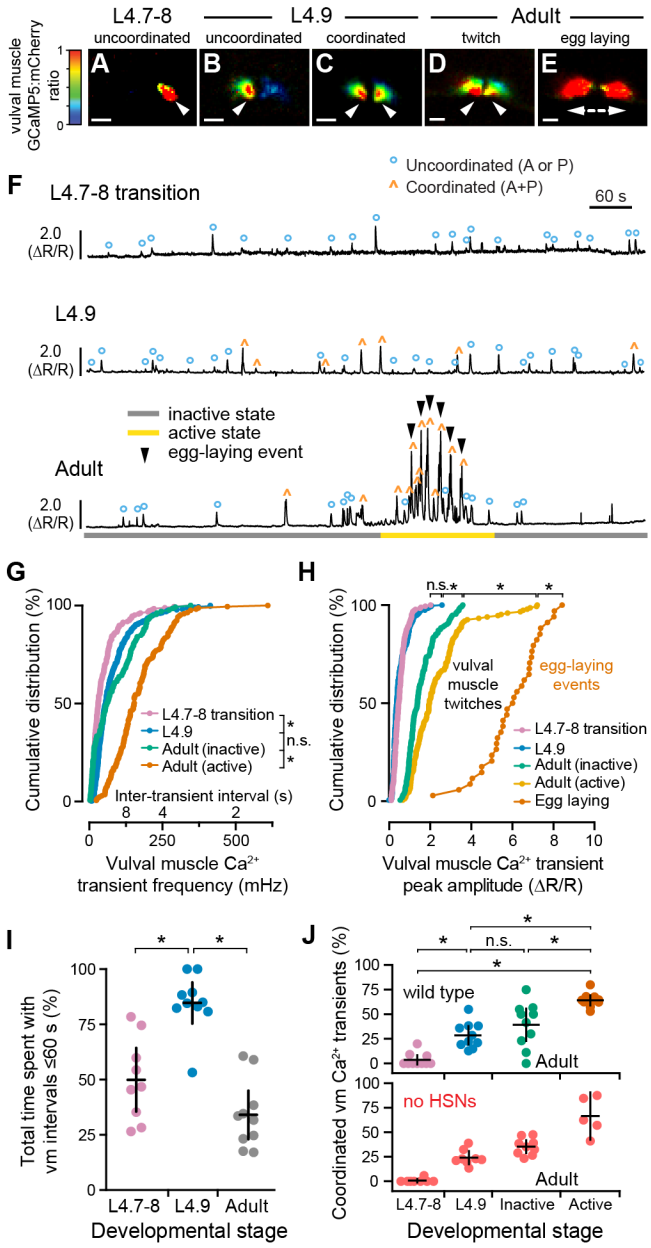

997

998 **Fig. 4. Development of coordinated vulval muscle Ca^{2+} transients in the L4.9 stage**
999 **does not require presynaptic HSN input.** (A-E) Micrographs of GCaMP5:mCherry
1000 fluorescence ratio during vulval muscle Ca^{2+} transients at the L4.7-8 (A), L4.9 larval
1001 stages (B,C), and during the adult active state (D,E). White arrowheads show localization
1002 of Ca^{2+} transients. Scale bars are 10 μm; anterior at left, ventral at bottom. See also
1003 Movies S3-6. (F) GCaMP5:mCherry (ΔR/R) ratio traces of vulval muscle Ca^{2+} activity at

1004 L4.7-8 (top), L4.9 (middle), and in adults (bottom) during distinct inactive (grey) and active
1005 (yellow) egg-laying states. Uncoordinated transients are indicated by blue circles (°),
1006 coordinated transients by orange carets (^), egg-laying events by black arrowheads. (G
1007 and H) Cumulative distribution plots of instantaneous vulval muscle Ca^{2+} transient peak
1008 frequencies (G) and amplitudes (H) at L4.7-8 (pink), L4.9 (blue), and in the egg-laying
1009 inactive (green) and active state (orange) of adults. Asterisks indicate $p<0.0001$; n.s.
1010 indicates $p>0.9999$ (Kruskal-Wallis test). (I) Scatterplots show time spent by 9-10 animals
1011 with frequent Ca^{2+} transients (inter-transient intervals ≤60 s) at L4.7-8 (pink), L4.9 (blue),
1012 and in adults (gray). Error bars show 95% confidence interval for the mean. Asterisks
1013 indicates $p\leq0.0002$ (one-way ANOVA). (J) Scatterplots show percent synchronous
1014 anterior and posterior vulval muscle Ca^{2+} transients in each individual at L4.7-8 (pink),
1015 L4.9 (blue), and in adult egg-laying inactive (green) and active states (orange) in wildtype
1016 (top) and *egl-1(n986dm)* animals (red) lacking HSNs (bottom). Error bars show 95%
1017 confidence intervals for the mean from ≥5 animals. Asterisks indicate $p\leq0.0022$; n.s.
1018 indicates $p\geq0.1653$ (one-way ANOVA).

1019

1020

1021

1022

1023

1024

1025

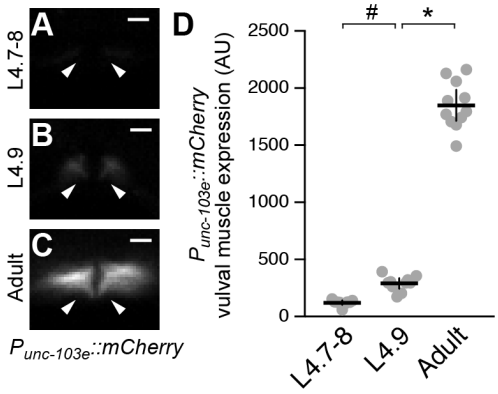

1026

1027 **Fig. 5. ERG expression in the vulval muscles increases during development.** (A-C)
1028 Micrographs of mCherry fluorescence in the vulval muscles from a *unc-103e* (ERG)
1029 transcriptional reporter in L4.7-8 (A) and L4.9 larval stages (B), and in adults (C). White
1030 arrowheads show anterior (left) and posterior (right) vulval muscle cells; scale bar is 10
1031 µm. (D) Scatterplots show mean mCherry fluorescence from the *unc-103e* promoter from
1032 ten animals at the L4.7-8, L4.9, and adult stages. Error bars show 95% confidence interval
1033 for the mean; '#' indicates p=0.0288 and asterisk indicates $p \leq 0.0001$ (one-way ANOVA).

1034

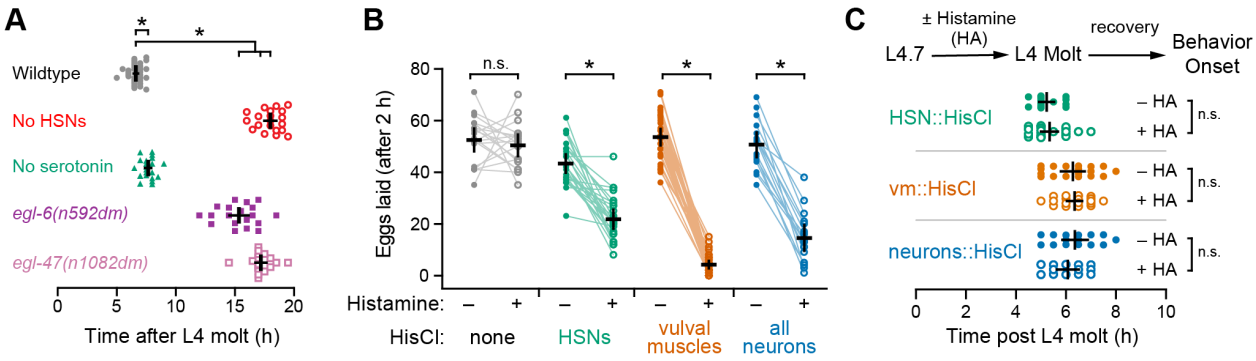

Fig. 6. Early HSN and vulval muscle activity is not required for the onset of egg-laying behavior. (A) Scatter plots of the first egg-laying event in wild-type (grey), HSN-deficient *egl-1(n986dm)* (red open circles), serotonin-deficient *tph-1(mg280)* (green triangles), *egl-6(n592dm)* (purple squares), and *egl-47(n1082dm)* (pink open squares) mutant animals. Error bars show 95% confidence intervals for the mean from ≥19 animals. Asterisks indicate $p \leq 0.0016$ (One-way ANOVA with Bonferroni correction for multiple comparisons). (B) Scatter plots showing eggs laid by three 24-hour adult animals in two hours before (closed circles) and in two hours after incubation on plates with 10 mM histamine (open circles). Transgenic animals expressing HisCl in vulval muscles (orange), HSN neurons (green), and all neurons (blue) were compared with the non-transgenic wild-type (grey). Error bars indicate 95% confidence intervals for the mean from ≥17 paired replicates. Asterisks indicate $p<0.0001$; n.s. indicate $p=0.5224$ (paired Student's t test). (C) Top, transgenic L4.7 animals were incubated on NGM plates with or without 10 mM histamine until the L4-Adult molt. Animals were then moved to plates lacking histamine and allowed to recover and lay eggs. Bottom, scatter plots show the timing of the first egg-laying event with (open circles) and without (closed circles) histamine. Error bars indicate 95% confidence intervals for the mean; n.s. indicates $p>0.9999$ (one-way ANOVA with Bonferroni correction for multiple comparisons).

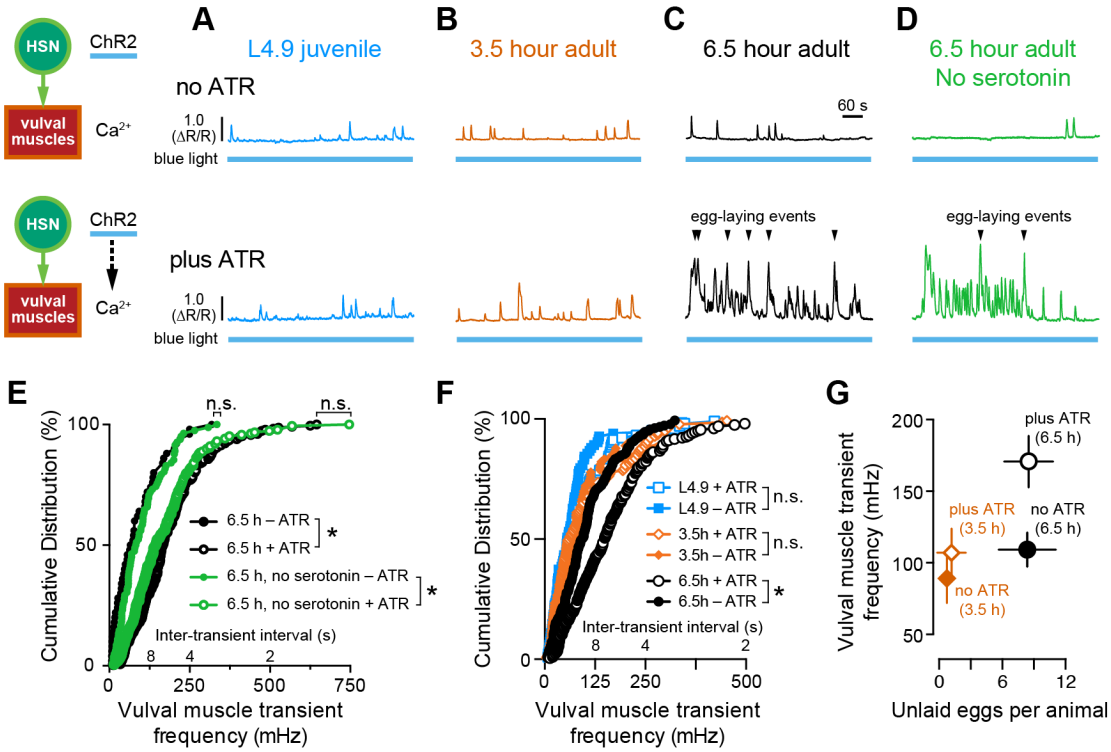

Fig. 7. Vulval muscle responsiveness to HSN activity increases as maturing animals accumulate unlaid eggs. (A-D) Traces of vulval muscle Ca^{2+} activity at the L4 stage (A, blue), 3.5-hour adults (B, orange), 6.5-hour wild-type adults (C, black), and 6.5-hour serotonin-deficient *tph-1(mg280)* mutant adults (D, green) with and without optogenetic activation of HSN. Animals were grown in the presence (plus ATR, top) or absence (no ATR, bottom) of all-*trans* retinal (see cartoon schematic). Continuous 489 nm laser light was used to simultaneously stimulate HSN ChR2 activity and excite GCaMP5 fluorescence for the entire recording. Arrowheads indicate egg-laying events. Blue bars under the Ca^{2+} traces indicate the period of continuous blue light exposure. (E) Cumulative distribution plots of instantaneous peak frequencies (and inter-transient intervals) of vulval muscle Ca^{2+} activity in 6.5-hour adult wild-type (black filled circles, no ATR; black open circles, plus ATR) and *tph-1(mg280)* mutant animals (green filled circles, no ATR; green open circles, plus ATR). Asterisks indicate $p<0.0001$; n.s. indicates

1068 $p \geq 0.2863$ (Kruskal-Wallis test with Dunn's correction for multiple comparisons). (F)
1069 Cumulative distribution plots of instantaneous peak frequencies (and inter-transient
1070 intervals) of vulval muscle Ca^{2+} activity in L4.9 juveniles (blue filled squares, no ATR; blue
1071 open squares, plus ATR), 3.5-hour old adults (orange filled circles, no ATR; orange open
1072 circles, plus ATR), and 6.5-hour old adults (black filled circles, no ATR; black open circles,
1073 plus ATR). Asterisk indicates $p < 0.0001$; n.s. indicates $p \geq 0.3836$ (Kruskal-Wallis test). (G)
1074 Plot shows the average number of unlaid eggs present in the uterus and the average
1075 vulval muscle Ca^{2+} transient peak frequency in 3.5-hour old adults (orange closed
1076 diamond, no ATR; orange open diamond, plus ATR), and 6.5-hour old adults (black
1077 closed diamond, no ATR; black open diamond plus ATR). Error bars indicate 95%
1078 confidence intervals for the means.

1079

1080

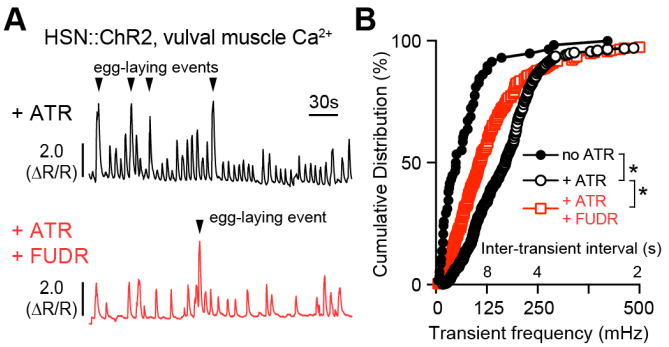

1081

1082 **Fig. 8. Sterilization decreases vulval muscle responsiveness to optogenetic HSN**
1083 **activation**. (A) Traces of HSN-induced vulval muscle Ca^{2+} activity in untreated (top,
1084 black) and FUDR-treated 24-hour adult animals (bottom, red). Arrowheads indicate egg-
1085 laying events. (B) Cumulative distribution plots of instantaneous peak frequencies (and
1086 inter-transient intervals) of vulval muscle Ca^{2+} activity after optogenetic activation of HSNs
1087 in untreated animals grown with ATR (+ATR, open black circles), FUDR-treated animals
1088 with ATR (+ATR, open red circles), and in untreated animals without ATR (no ATR, closed
1089 black circles). Asterisks indicate $p<0.0001$ (Kruskal-Wallis test with Dunn's correction for
1090 multiple comparisons).

1091

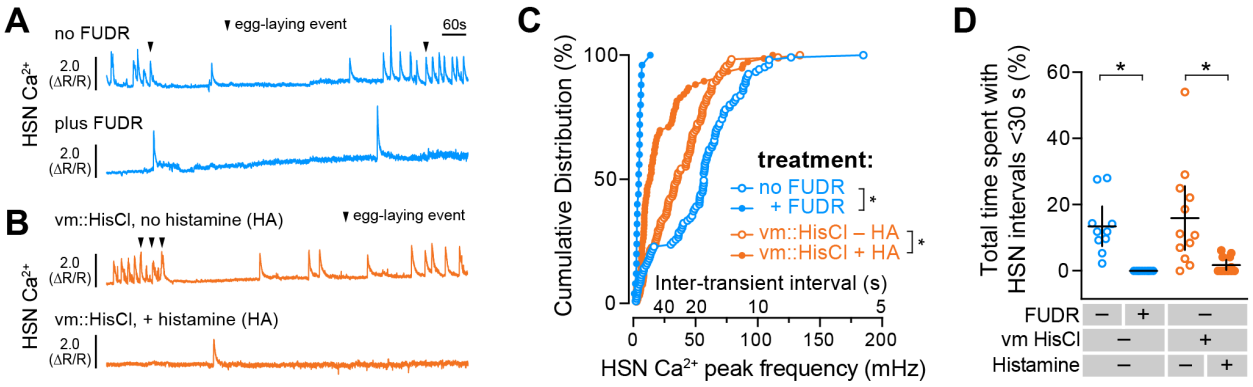

Fig. 9. Egg accumulation and postsynaptic vulval muscle activity promote presynaptic HSN activity. (A) HSN Ca^{2+} traces in untreated (top) and FUDR-treated (bottom) adult animals. (B) HSN Ca^{2} traces in adult animals expressing HisCl in the vulval muscles (vm) without (top) and after 10 mM histamine treatment (bottom). Arrowheads indicate egg-laying events. (C) Cumulative distribution plots of instantaneous HSN Ca^{2+} transient peak frequencies (and inter-transient intervals) of adult HSN Ca^{2+} activity. (D*)* Scatterplots show total time spent by each individual with HSN transients ≤30s apart in FUDR (blue open circles), FUDR-treated (blue closed circles), no histamine (orange open circles), and histamine-silenced vulval muscles (orange closed circles). Asterisks indicate $p \leq 0.0031$ (Kruskal-Wallis test). Error bars indicate 95% confidence intervals for the mean.

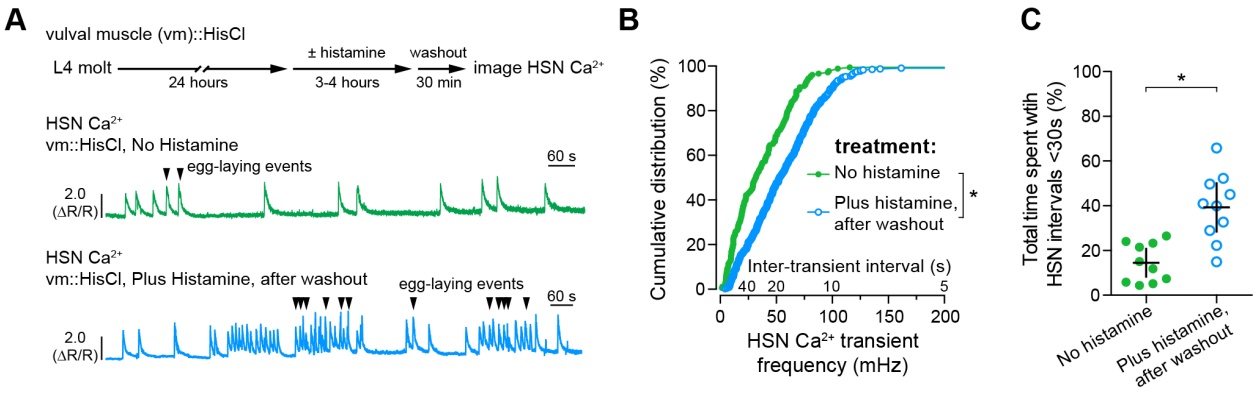

Fig. 10. Egg accumulation drives a homeostatic increase in HSN activity and egg release. (A) 24-hour old adult animals expressing HisCl in the postsynaptic vulval muscles (vm) and GCaMP5/mCherry in the presynaptic HSNs were placed onto NGM plates with (blue, bottom) or without histamine (green, top) for 3-4 hours to induce muscle silencing and cessation of egg laying. Animals were then moved to plates without histamine and allowed to recover for 30 minutes before HSN Ca^{2+} imaging. Arrowheads indicate egg laying events. (B) Cumulative distribution plots of instantaneous HSN Ca^{2+} transient peak frequencies (and inter-transient intervals) after histamine washout (blue open circles) compared with untreated controls (green closed circles). Asterisks indicate $p<0.0001$ (Mann-Whitney test). (C) Scatter plots show fraction of time spent by each individual with frequent HSN Ca^{2+} transients characteristic of the egg-laying active state (<30 s) in untreated controls (green circles) and after histamine washout (blue open circles). Error bars indicate 95% confidence intervals for the mean. Asterisk indicates $p=0.0005$ (Student's t test).

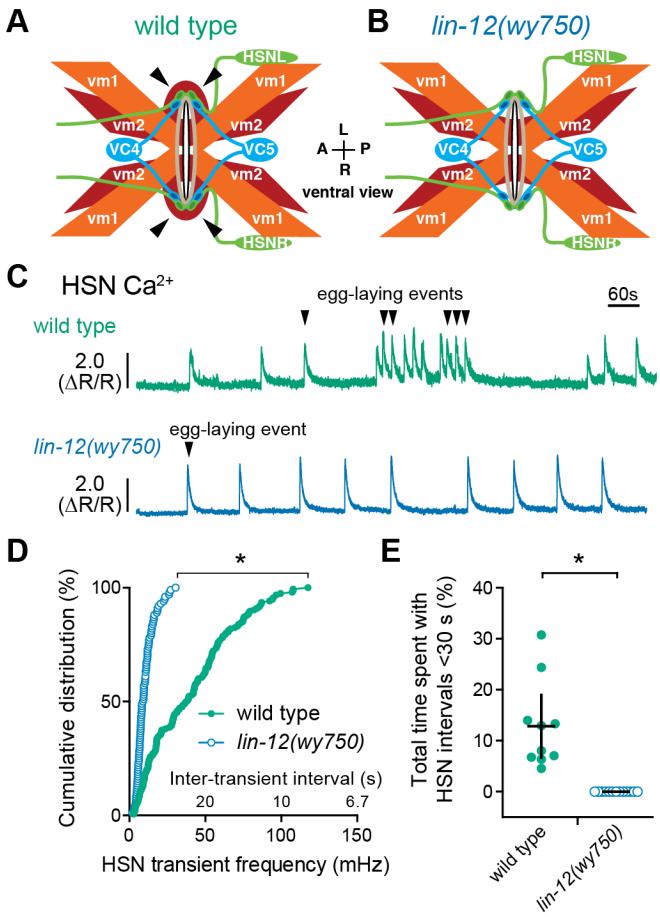

1120

1121 **Fig. 11: The vm2 muscle arms are required for vulval muscle feedback to HSN and**
1122 **burst firing.** (A-B) Cartoon of egg-laying circuit structure (lateral view) in wild-type (A)
1123 and *lin-12(wy750)* mutant (B) animals missing lateral vm2 muscle arms (arrowheads). (C)
1124 Traces show HSN Ca^{2+} activity in wild-type (green) and *lin-12(wy750)* mutant animals
1125 (blue). Arrowheads indicate egg-laying events. (D) Cumulative distribution plots of
1126 instantaneous Ca^{2+} transient peak frequencies (and inter-transient intervals) in wild-type
1127 (green circles) and *lin-12(wy750)* mutants (blue circles). Asterisks indicate $p<0.0001$
1128 (Mann Whitney test). (E) Scatter plots show fraction of time spent by each individual with
1129 frequent HSN Ca^{2+} transients characteristic of the egg-laying active state (<30 s) in wild-
1130 type (green circles) and *lin-12(wy750)* mutant animals (blue open circles). Error bars

1131 indicate 95% confidence intervals for the mean. Asterisk indicates p=0.0011 (Student's t

1132 test).

1133

1134

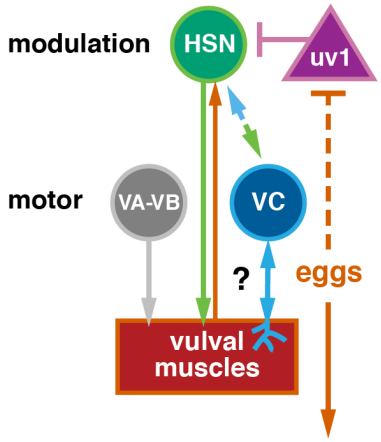

1135

1136 **Fig. 12**: Working model of how retrograde signals from the postsynaptic vulval muscles
1137 (question mark) might directly or indirectly modulate burst firing in the presynaptic HSNs.
1138 HSN is a serotonergic and peptidergic modulatory neuron that synapses onto the vulval
1139 muscles and the VC motor neurons. VA, VB, and VC are cholinergic motor neurons that
1140 synapse onto the vulval muscles. uv1 is a tyraminergic and peptidergic neuroendocrine
1141 cell mechanically activated by egg release that then feedback inhibits HSN. Arrows
1142 indicate activation, bar-headed lines indicate inhibition; see text for more details.

1143

1144 **Movie legends**

1145 Movie 1. Ratio recording of a HSN Ca^{2+} transient at the L4.9 larval stage. High Ca^{2+} is
1146 indicated in red while low calcium is in blue. The HSN cell body and pre-synaptic terminal
1147 are indicated. Head is at bottom, tail is at left.

1148 Movie 2. Ratio recording of a HSN Ca^{2+} transient prior to an egg-laying event in an adult
1149 animal during the active state. High Ca^{2+} is indicated in red while low calcium is in blue.
1150 The HSN cell body and pre-synaptic terminal are indicated. Head is at bottom, tail is at
1151 top.

1152 Movie3. Ratio recording of an uncoordinated vulval muscle Ca^{2+} transient at the L4.7-8
1153 larval stage. High Ca^{2+} is indicated in red while low calcium is in blue. Developing anterior
1154 and posterior vulval muscles are indicated. Head is at top, tail is at bottom.

1155 Movie 4. Ratio recording of an uncoordinated vulval muscle Ca^{2+} transient at the L4.9
1156 larval stage. High Ca^{2+} is indicated in red while low calcium is in blue. Anterior and
1157 posterior vulval muscles are indicated. Head is at left, tail is at bottom.

1158 Movie 5. Ratio recording of a coordinated vulval muscle Ca^{2+} transient at the L4.9 larval
1159 stage. High Ca^{2+} is indicated in red while low calcium is in blue. Anterior and posterior
1160 vulval muscles are indicated. Head is at top, tail is at bottom.

1161 Movie 6. Ratio recording of coordinated vulval muscle Ca^{2+} transients during egg laying
1162 in adult animals. High Ca^{2+} is indicated in red while low calcium is in blue. The anterior
1163 and posterior vulval muscles are indicated along with a previously laid egg. Head is at
1164 right, tail is at left.